Impact of Geological Conceptualization on the Calibration of Groundwater Models at the Mannheim Wellfield, Kitchener, Ontario

by

Xin Tong

A thesis

presented to the University of Waterloo

in fulfillment of the

thesis requirement for the degree of

Master of Science

in

Earth Science

Waterloo, Ontario, Canada

Author’s Declaration

I hereby declare that I am the sole author of this thesis. This is a true copy of the thesis, including any required final revisions, as accepted by my examiners.

I understand that my thesis may be made electronically available to the public.

Abstract

This study investigates the importance of geological data on the calibration of groundwater models using long term pumping/injection and monitoring well records at a wellfield in the Region of Waterloo, Ontario. Four different geological models with homogeneous geological layers are calibrated by coupling HydroGeoSphere (HGS) and the parameter estimation code PEST using water-level variation records collected during municipal well operations. The estimated hydraulic conductivity (K) and specific storage (S_S) are consistent to those obtained through previous aquifer tests. The four geological models are well calibrated with assigned initial K and S_S and yield reliable estimates for the upper layers where most data points are collected. However, the K and S_S estimated for lower layers with fewer observation points vary more significantly among the models. The comparison of simulated and observed drawdown for both model calibration and validation reveals that all four groundwater flow models with varying geology can capture the water-level fluctuation pattern quite well. However, these models fail to capture the rapid water- level variations at some wells. This study demonstrates the usefulness of water level fluctuation data resulting from municipal well operations in the calibration of groundwater flow models.

Acknowledgements

I would like to thank my supervisor Professor Walter A. Illman for giving me this opportunity to work on this project. I benefit a lot from his expertise, patience and dedication, especially his guidance and assistance on my writing.

I would like to thank my committee members Dr. David Rudolph and Dr. Steven Berg, for their generous time, comments and support that greatly improved my thesis project. Special thanks to Dr. Steven Berg and Aquanty Inc for providing the software HydroGeoSphere license and technical supports.

Thanks to the Regional Municipality of Waterloo for providing funding to the project. I would like to thank Tammy Middleton and Emily Ballent for being open to information sharing and experienced help throughout this project.

I would like to thank my colleagues and friends for their support, who include Ning Luo, Chao Zhuang, Zhanfeng Zhao, Young-Jin Park, Jiabao Zhu, Shuai Yang, Zeren Ning and Violet Huang.

Table of Contents

List of Figures

List of Tables

1. Introduction

The Region of Waterloo (RoW) in Ontario, Canada is one of the largest municipalities in Canada that relies mostly (> 75%) on groundwater supplies for its drinking water. The dramatic growth of the region and the increasing water demand promote the development of municipal wellfields as well as the need to sustainably manage the groundwater resource.

There are more than 40 wellfields consisting of more than 120 wells within the region which supply in excess of 269,000 m^3/day of groundwater to urban citizens (Lake Erie Region Source Protection Committee, 2012). The groundwater is extracted from a complex multi-aquifer-aquitard system within the Waterloo Moraine, which was formed by interlobate glacial activity, with seven well fields having wells screened in the upper aquifers (AFB1 and AFB2) and ten well fields are screened in the older deposits (Bajc and Shirota, 2007).

The complexity and susceptibility of the Waterloo Moraine to overexploitation of groundwater resources and its potential contamination requires the sound understanding of hydrogeology, including the reliable estimation of hydraulic parameters such as hydraulic conductivity (K) and specific storage (S_S). A number of hydraulic parameter estimation approaches have been developed and studied during the past several decades include: (1) the analysis of small scale data including grain size distribution (Hazen, 1911; Kozeny, 1927; Shepherd, 1989), collection of core samples for laboratory permeameter analyses (Sudicky, 1986; Freeze and Cherry, 1979; Sudicky et al., 2010; Alexander et al., 2011), slug tests (Hvorslev, 1951; Bouwer and Rice, 1976;

Cooper et al., 1976; Rehfeldt et al., 1992; Mas-Pla et al., 1997); and (2) performing pumping tests and fitting data to analytical solutions to determine the large-scale hydraulic properties of the aquifer (Theis, 1935; Cooper and Jacob, 1946; Chen et al., 2003). However, the large area of the municipal well fields raises the question whether small scale hydraulic parameter estimates are reliable in predicting water levels and groundwater flow. Another concern is that it is difficult to conduct dedicated pumping tests within a municipal well field where pumping/injection schedules cannot be readily modified or terminated. When dedicated pumping tests can be conducted, existing analytical solutions that treat the subsurface to be homogeneous are typically utilized, which yields biased and questionable parameter estimates (Wu et al., 2005; Berg and Illman, 2011a, b; 2013, 2015).

There are monitoring networks installed within municipal wellfields to manage groundwater demand and usage. Other than designing proper pumping/injection rates of water supply boreholes, these monitoring data can potentially be used to better characterize regional groundwater flow and estimate hydraulic parameters (Yeh and Lee 2007; Harp and Vesselinov 2011).

In a previous study (Luo and Illman, 2016), these long-term pumping/ injection events and water-level variation records were used to estimate hydraulic parameters including transmissivity (T) and storativity (S) for the shallow aquifer (AFB2) within the Waterloo Moraine. A set of T and S values were estimated between each production and monitoring borehole by fingerprinting the water-level variations to pumping/injection rate changes. The fingerprinting process was accomplished through

the Theis (1935) model implemented in the WELLS code (Mishra and Vesselinov, 2011) coupled with a nonlinear parameter estimation code PEST (Doherty, 2005). This study showed that long-term municipal water-level records were amenable for hydraulic parameter estimation as the geometric means of the individual T and S estimates were similar with previous pumping tests at the study site. However, the wide range of estimated T (9 - 55,335 m/day) and S (0.002 - 0.736) indicated the high heterogeneity of the investigated aquifer. In addition, the S values estimated in the study are significantly larger than those typically estimated for in confined aquifers which may be due to the utilization of the Theis (1935) solution since the Theis (1935) solution neglects borehole storage effects. When the effects of borehole storage are not considered in pumping and observation boreholes, the estimated S values could be several orders of magnitude larger (Dames and Moore, 1990). The borehole storage effect can become significant especially when water-supply boreholes have large diameters and monitoring wells very close to the water-supply wells. Furthermore, poor validation results using data that were not used for calibration purposes suggested that T and S estimates from individual pumping and monitoring boreholes may not be suitable for the drawdown prediction of other monitoring wells. In order to increase the accuracy of parameter estimates at this site, Luo and Illman (2016) concluded that a more sophisticated groundwater flow model that considers the heterogeneity as well as better accounting of the forcing functions (i.e., initial and boundary conditions as well as source/sink terms) is needed.

There are a number of approaches to map the K heterogeneity. A conceptually

simple approach is to map the K heterogeneity through the interpolation of small-scale K estimates including permeameter tests, slug tests and single-hole tests, but a large number of data is required. For example, Rehfeldt et al. (1992) estimated that about 400,000 K measurements would be required to accurately predict the transport of tracers in an alluvial aquifer at the MADE site. Thus, it will be expensive and time-consuming to perform such analyses at a municipal wellfield.

Geostatistical and stochastic inverse approaches are also an alternative way to map K heterogeneity (e.g., Kitanidis and Vomvoris, 1983; Rubin and Dagan, 1987; Yeh et al., 1996; Riva et al., 2009). This approach can produce statistical moments of hydraulic variables including uncertainty maps to better represent the accuracy of estimated hydraulic parameters.

Recently, hydraulic tomography (HT), which is designed to incorporate hydraulic head recorded at multiple locations for model calibration from sequential pumping tests, has been developed as a useful tool to delineate subsurface heterogeneity and has been tested under synthetic, laboratory, and field conditions (e.g., Yeh and Liu, 2000; Bohling et al., 2002; Illman et al., 2007, 2008, 2009, 2010 a, b; 2012; Berg and Illman, 2011 a, b; Cardiff et al., 2013 a, b; Illman et al., 2015; Zhao et al., 2016; Zhao and Illman, 2017). However, HT has not been applied at municipal wellfields since sequential pumping tests may be difficult to perform. In order to overcome this difficulty, long-term pumping/ injection events and water-level variation records are used in this study to jointly calibrate a groundwater flow model consisting of homogeneous geological units to estimate the K and S_S. As mentioned by Berg and

Illman (2015), this is a form of HT. As an initial attempt, geological models are used for the HT analyses in this study as previous studies have shown the importance of geological data in obtaining more realistic hydraulic parameter estimates (Illman et al., 2015; Zhao et al., 2016; Luo et al., 2017; Zhao and Illman, 2017; Zhao and Illman, 2018).

Illman et al. (2015) compared the performance of HT based on the effective parameter, geological and geostatistical approaches, and the results showed that the geostatistical inversion approach preformed the best, but HT based on a geological model with perfect knowledge of stratigraphy came a close second. Moreover, the geological model performed even better than the geostatistical approach when the number of observation data and the number of pumping tests were reduced. This was due to the fact that the geological model incorporated soft data (i.e. stratigraphy), while the geostatistical approach assumed a homogenous hydraulic parameter field as an initial guess. The most robust results were obtained when geological information was included in the geostatistical inversion approach. However, since perfect knowledge of stratigraphy is not available in the field, there is a critical need to assess the impact of various conceptualizations of site geology on groundwater model calibration and HT at the field scale.

Geological uncertainty in groundwater modeling normally originates from (a) the geological structure; (b) the use of effective model parameters; and (c) model parameters including local scale heterogeneity (Refsgaard et al., 2012). Zhao et al. (2016) compared the performance of four geological models of different accuracies

using laboratory sandbox data by model calibration and validation. Results revealed that geological models with accurate knowledge of stratigraphy and with errors in stratigraphy both were well calibrated because of the parametric compensation effect introduced through calibration caused by model structure error (Refsgaard et al., 2012), but the use of inaccurate geological data led to unrealistic parameter estimates in some geological units and poor model validation results. Thus, while an inaccurate model could be well calibrated, this does not necessary result in a robust model that is suitable for making accurate predictions of groundwater flow.

The overall goal of this study is to examine the impact of different geological conceptualization on the calibration of groundwater models at a wellfield where long term pumping/injection and monitoring well records are available for HT technology application. Specifically, the objectives of the study are to: 1) demonstrate the usefulness of long-term pumping/injection and monitoring well records obtained through municipal well field operations for estimating hydraulic parameters (i.e., K and S_S) of geological units; 2) investigate the impact of different geological conceptualization on the performance of groundwater model calibration and validation; and 3) explore the importance of geological data in improving the results of HT analysis at a large-scale field site.

2. Site description and geology

This study focuses on the Mannheim East Municipal Well Field located in the southwest area of the city of Kitchener, Ontario, Canada. In order to minimize the effect

of boundary conditions on simulating groundwater flow, the model is constructed in a larger area (5 km × 5 km) with the Mannheim East Well Field located approximately in the center of the simulation domain.

Figure 1 illustrates the distribution of boreholes utilized in this study. There are 13 water-supply wells (K21, K25, K29, K91, K92, K93, K94, ASR1, ASR2, ASR3, ASR4, RCW1, and RCW2) and 19 monitoring wells with 28 screens completed at various depths (ow16-60, ow23a-65, ow2-09, ow1-10, ow3-85, ow5ab-89, ow8ab-89, ow10ab-89, ow1a-96, ow1cd-96, ow2ab-96, ow4ab-96, ow1ab-02, ow2ab-02, ow3ab- 02, ow5-02, ow1-08, ow3-09, and ow4-09) within the study area. A detailed description of these wells is provided in Table 1. These wells are subdivided into three smaller well fields for various purposes within the Mannheim East Well Field and they consist of Mannheim East, Peaking and Aquifer Storage and Recovery (ASR) sites, located within the core area of the Waterloo Moraine.

The Waterloo Moraine is a quaternary kame and kettle complex formed by numerous advances and retreats of ice lobes during the Wisconsinan glaciation, which has been studied extensively by Karrow (1993). The resulting glaciofluvial sediments consist of a variety of materials including clay, interbedded tills, fine sand, sandy gravel, and coarse gravel, which are normally stratified and poorly sorted (Martin and Frind, 1998; Golder Associates, 2011).

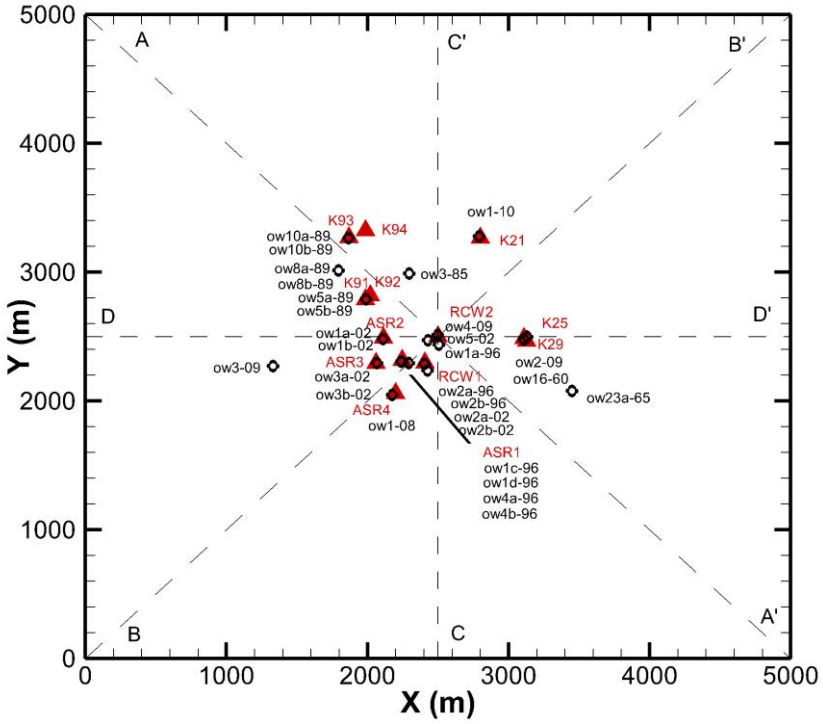

Fig. 1 The distribution of water-supply and monitoring boreholes in the study area. The red triangles indicate the water-supply wells and the black circles indicate the water-monitoring boreholes.

There are four relatively continuous till units that are identified within the Moraine, including Pre-Catfish Creek Tills, Catfish Creek Till, Maryhill Till and Tavistock/Pork Stanley Till. The Pre-Catfish Creek Tills, which is the first till units deposited in the area, are generally hard, stony silts to clayey silt tills (Karrow, 1993). These till units, including Canning Till and several other tills, were formed during the Wisconsinan glacial events and locally overlie the bedrock (Martin and Frind, 1998).

The Catfish Creek Till, which is the next oldest unit, were deposited by a major glacial advance across southern Ontario, is an extremely dense, stony silt till and commonly referred to as “hardpan” by local experienced water well drillers (Golder Associates, 2011).

The Maryhill Till, separates the upper and the deeper aquifer, is a clay-rich low permeability natural infiltration barrier. Previous studies have identified three separate ice advances which resulted in the an Upper, Middle and Lower Maryhill Till (Karrow, 1993; Paloschi, 1993; Bajc and Shirota, 2007).

The youngest till units, Tavistock/Pork Stanley Till, overlie large portions of the upper aquifer. The Tavistock Till is a dark brown clayey silt till, similar to the Maryhill Till, while the Port Stanley Till is recognized as a sandy silt to silty sand till (Golder Associates, 2011).

3. Description of geological models

Modeling can provide valuable insights on the Waterloo Moraine groundwater system and practical advice for source water protection and management for the Waterloo Region. As models evolved from a simple, layer-cake concept to a fully three -dimensional (3D) distribution of geological units, the focus has changed in scale from the well scale to the scale of the entire Waterloo Moraine system to solve more sophisticated problems such as the assessment of well vulnerability and wellhead protection areas (Frind et al., 2014).

One of the first groundwater flow model of the Waterloo Moraine was developed as a simple, two-dimensional (2D), finite element, layer-cake system by Emil Frind in 1973 (International Water Supply Ltd, 1973). The model was calibrated to hydraulic head values at different observation wells and then used for the prediction of aquifer responses under various pumping conditions.

A quasi-3D model was then successfully developed and utilized by Rudolph (1985) and Rudolph and Sudicky (1990) at the Greenbrook well field to capture the complexity of the Waterloo Moraine system.

The Waterloo North Aquifer System Study (Terraqua Investigation Ltd, 1992) and the Study of the Hydrogeology of the Waterloo Moraine (Terraqua Investigation Ltd, 1995) were conducted to define the major aquifer and aquitard units and regional recharge zones.

Then, a fully 3D Waterloo Moraine model was created by Martin and Frind (1998) based on the application of WATFLOW (Molson et al., 1995). The groundwater model utilized triangular, prismatic, finite elements and allowed for grid refinement, which resulted in the better handling of complex geometries and representation of irregular and sloping layers (Callow, 1996). The boundaries of the model were defined as natural features including rivers, creeks, and swamps, which would not be affected by pumping events.

Bajc and Shirota (2007) constructed a new geological model of the Waterloo Moraine, applying a basin analysis approach to data collection and interpretation, which provided details to various geological units, including information on the distribution, thickness, geometry and other attributes. The model was built mainly based on geological information and the subsurface sediment structure including geological and geophysical data from a regional borehole data base (Farvolden et al., 1987; Bajc and Newton, 2007), published information on the Quaternary geology, downhole geophysical logs, and identification of available sediment exposures. Since

hydrogeological data including hydraulic head and hydraulic test observation data were not used in the model layer interpretation, the model layers were considered stratigraphic layers, which may not be consistent with hydrogeological data at each well field (Blackport et al., 2014). Refinements to this model were made within various municipal well fields through subsequent studies (Stantec Consulting Ltd, 2009, 2012a, 2012b, 2012c; Golder Associates Ltd, 2011; Blackport Hydrogeology Inc, 2012a, 2012b; Matrix and SSPA, 2014a, b).

Although it is clear that different geological conceptualizations will affect the results of groundwater flow model calibration and validation results, no known studies on HT have been conducted that utilize long-term municipal well records.

In this study, a new geological model was constructed based on the lithology of wells installed within the study area using Leapfrog Geo (ARANZ Geo Ltd.). Leapfrog Geo constructs 3D geological models using borehole records and GIS data based on the Fast Radial Basis Function method. In total, the lithology information from 250 wells were utilized for the construction of the new geological model. The distribution of these borehole records at the study site is illustrated in figure 2 (b). For each borehole record, lithology information was obtained from the WRAS+ database (Regional Municipal of Waterloo, 2014) and summarized based on the three main materials identified for each core sample. In total, 11 groups of geological units are identified based on the conceptual hydrogeologic model of the Waterloo Moraine constructed by Bajc and Shirota (2007) and Matrix and SSPA (2014a, b). The nomenclature of Ontario Geological Survey (OGS) is adopted here for layer identification, in which AT refers

to an aquitard, while AF refers to an aquifer. Following AT or AF, letters and numbers are used to identify the sequence of units, with “A” as the youngest grouped sequence followed by “B” and “1” as the youngest unit in the group followed by “2.

Figure 2 shows the resul ting 3D geological model with four cross-section maps. The dimension of the geological model is 5 km × 5 km in X (east) and Y (north) directions with an elevation of 200 masl as the bottom and the topography as the top. The bottom of the model is set at 200 masl because no data is available below 200 masl and all the investigated aquifer layers are located above 200 masl. In total, 11 geological layers were identified, which are ATB1, AFB1, ATB2, AFB2, ATB3, ATC1, AFC1, ATE1, AFF1, ATG1 and Bedrock from the top to the bottom.

In comparison to the conceptual hydrogeologic model of the Waterloo Moraine, some layers were merged (ATC1 and ATC2 were combined as ATC1 and AFF1 and AFD1 were combined as AFF1) in the newly constructed geological model. This is because: 1) these geological layers are thin in thickness and consist of similar materials, and 2) they are located at low elevations where geological data from borehole logs are limited in order for one to accurately separate these layers.

Examination of Figure 2 reveals that ATB1 is a thin and patchy aquitard that lies on top of the study area, while AFB1 is an unconfined aquifer present throughout the study area with considerable recharge from precipitation that appears to take place in the central and eastern portion of the site. ATB2 is a thin aquitard that separates AFB2 and AFB1 in most of the study area. AFB2 is the primary water-supply aquifer in the Mannheim East wellfield. The AFB2 aquifer is evident in the central area of the study

site, where the municipal well field was developed with a maximum thickness of approximately 40 m. However, the thickness decreases as it extends to the edges of the geological model. Beneath the AFB2 aquifer, the ATB3 aquitard is continuous across the study area followed by the aquitard ATC1. These two aquitards with extremely low permeability separate the upper aquifers (AFB1 and AFB2) to the lower aquifer/aquitard system. Between the ATC1 aquitard and the bedrock, four geological layers (AFC1, ATE1, AFF1, and ATG1) have been further identified. These layers are found to be thin and discontinuous within the study area.

A simplified geological model has been developed by merging some of the layers with similar material, specifically ATB1 as AT1, AFB1, ATB2 and AFB2 as AF1, ATB3 and ATC1 as AT2, AFC1, ATE1, and AFF1 as AF2, ATG1 and Bedrock as AT3 (shown in Table 2). The five-layer geological model mainly reflects the contrast in the low and high *K* zones, while the 11-layer geological model incorporates more detailed stratigraphy information.

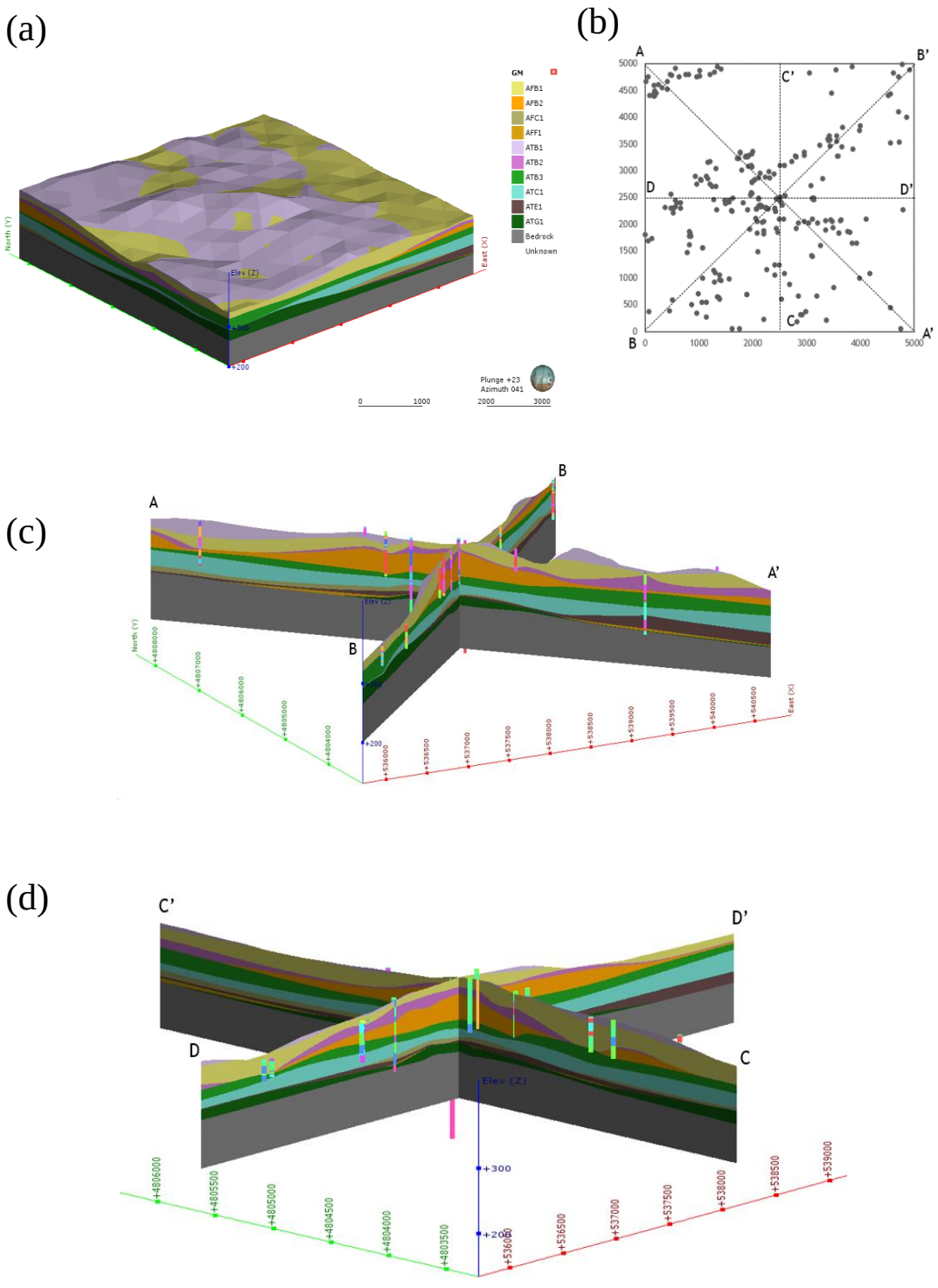

Fig. 2 (a) Constructed 3D geological model of the site using Leapfrog Geo. (b) Distribution of selected wells within the study area along with locations where cross sections are provided. (c) Cross-sections along A- A' and B-B'. (d) Cross-sections along C-C' and D-D'.

Two additional models are used in the study for groundwater flow model calibration and validation, including the Waterloo model, built by Bajc and Shirota (2007), and the Regional model (Matrix and SSPA, 2014a, b), refined based on the Waterloo Model. The Waterloo Model is constructed based on the subsurface information from RMOW (Regional Municipality of Waterloo) monitoring wells, urban geological database, field mapping data, cored boreholes, MOE (Ministry of the Environment) water well records and geophysical databases, while refinements are made to the Regional model with available hydrogeological data including municipal pumping data, hydraulic head data, water quality data, isotopic data, and well field shutdown data (Blackport et al., 2014). Compared with these large-scale models, the 11-layer geological model built in this study provides a high-resolution representation of local heterogeneity and hydraulic connectivity for the system.

In total, four geological models are utilized in this study including: (1) the 11-layer model; (2) the 5-layer model; (3) the Waterloo model; and (4) the Regional model for model calibration as well as model validation. The detailed layer information of each model is provided in Table 2 and cross-sections of each model with screen information are shown in Figure 3. The 11-layer geological model, the Waterloo model and the Regional model all divide the study domain into 11-layers, with main differences in the layer thickness of upper aquifer/aquitard and layer classification of the lower aquifer/aquitard.

The screen midpoints of all water-supply wells are located between 315 masl to 325 masl, while the screen midpoints of water-monitoring boreholes are located

between 185.82 masl and 368.88 masl. The screen of both water-supply wells and water-monitoring wells are mainly located at the bottom of AFB2, with few wells installed at AFB1, AFC1 and Bedrock based on the 11-layer geological model.

Although the depths of the screened intervals vary widely, well screens installed in AFB1, AFC1 and Bedrock lack constant monitoring records based on Table 1 with less than 40 data points available through the year of 2013. In addition, there are a large number of water level measurements in many wells, but in some wells, the monitoring record is quite sparse. Most wells are located at the bottom of AFB2 for both the 11-layer geological model and the Regional model, but at the bottom of AFB2/upper and middle of ATB3 for the Waterloo model. The classifications of upper layers are quite similar among four geological models, but the classifications of lower layers are dramatically different. The location of ow1c-96 is at AFC1 for the 11-layer geological model, at ATG1 for the Waterloo model, and ATC1 for the Regional model.

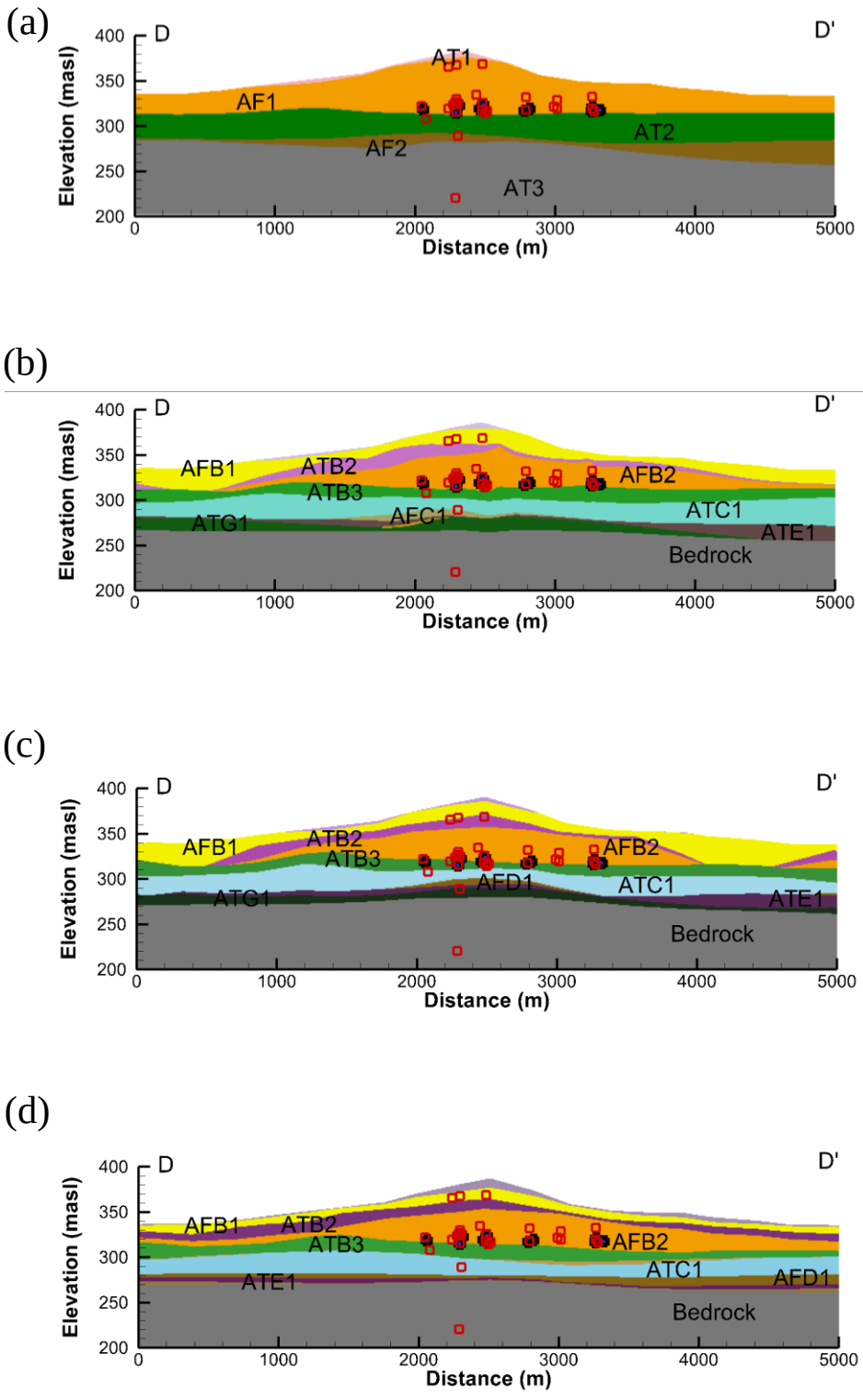

Fig. 3 Cross-sections along D-D' for (a) the 5-layer geological model; (b) the 11-layer geological model; (c) the Waterloo model; and (d) the Regional model with screen midpoint elevation information. The black circles indicate the water- supply wells and the red squares indicate the monitoring boreholes.

4. Data used for groundwater flow model calibration and validation

In this study, the same dataset obtained by Luo and Illman (2016) from the RoW are utilized, but the groundwater flow model calibration is conducted with data over a shorter time period. In particular, pumping/injection rate records in K- and ASR-series boreholes from January 1, 2005 to December 31, 2013 were utilized by Luo and Illman (2016), while the pumping/injection rates and water-level records collected during the year of 2013 are selected in this study to achieve computational efficiency.

Pumping/injection rate records from 13 water-supply wells (K21, K25, K29, K91, K92, K93, K94, ASR1, ASR2, ASR3, ASR4, RCW1, and RCW2) and water-level records from 19 monitoring locations with 28 screens at different depths (ow16-60, ow23a-65, ow2-09, ow1- 10, ow3-85, ow5ab-89, ow8ab-89, ow10ab-89, ow1a-96, ow1cd-96, ow2ab-96, ow4ab-96, ow1ab-02, ow2ab-02, ow3ab-02, ow5-02, ow1-08, ow3-09, and ow4-09) during the year of 2013 are obtained from the WRAS+ database for groundwater model flow calibration. Due to the use of numerical models for model calibration, pumping/injection rates in water-supply wells are expressed as daily pumped volume in m^3. In reality, pumping/ injection events normally operate for a couple of hours throughout a single day. However, the accurate operation time is not provided, thus the pumping/ injection rates are simplified as daily pumping/ injection rates. Therefore, for each water-supply well, 365 records are extracted from the database within the selected period. It should be noted that pumping/injection rates in these water-supply wells are not constant; instead, they vary frequently in most wells.

Water levels in water-supply and monitoring wells are measured manually and

electronically with pressure transducers. The transducers automatically record the water level every hour, thus the data recorded at the beginning of each day (12:00 am) are used as the water level for each day. At some wells, water levels are recorded monthly or bi-monthly through manual measurements, so the available data range from 3 to 12 in 2013.

Table 1 summarizes the number of data points used from each well for model calibration as well as model validation. All the water-supply wells are electronically measured, thus 365 data points are available for 2013. Groundwater levels in monitoring wells are measured either manually or electronically, thus the number of data ranges from 3 to 365 in 2013.

Since groundwater is constantly pumped or injected from water- supply wells, the initial water level is unknown for each screen. Based on the comparison of simulated and measured drawdown using empirical hydraulic parameters for various geological models during the forward simulation process, the simulated drawdown curves were fit well with the measured drawdown data after 20 days for most of monitoring wells. Therefore, the first 20 data points from monitoring wells are not used for model calibration and validation in order to simulate water fluctuation as a result of various pumping/injection events. The same strategy was applied by Luo and Illman (2016), which provided optimal matching between simulated and observed data. In total, 4985 data points are used for model calibration and 5085 data points are used for model validation in this study. Data from January to June 2013 are used for model calibration, while data from July to December 2013 are used for model validation.

Table 1 Summary of water-supply and water-level monitoring borehole information used for analysis.

Borehole type	Subdivided well sites	Well ID	Elevation of screen midpoint	Screened unit	Data point used for calibration	Data point used for validation
Water supply	Mannheim East	K21	316.55	AFB2	181	184
		K25	319.82	AFB2	181	184
		K29	319.28	AFB2	181	184
	Peaking	K91	317.06	AFB2	181	184
		K92	319.07	AFB2	181	184
		k93	320.45	AFB2	181	184
		K94	317.72	AFB2	181	184
	ASR	ASR1	322.50	AFB2	181	184
		ASR2	323.57	AFB2	181	184
		ASR3	323.41	AFB2	181	184
		ASR4	318.34	AFB2	181	184
		RCW1	314.76	AFB2	181	184
		RCW2	315.72	AFB2	181	184
Water- level monitoring	Mannheim East	ow1-10	316.37	AFB2	161	165
		ow16-60	314.38	AFB2	6	6
		ow2-09	317.85	AFB2	161	165
		ow23a-65	307.96	ATB3	161	165
	Peaking	ow3-85	321.81	AFB2	161	165
		ow5a-89	318.12	AFB2	161	165
		ow5b-89	331.92	AFB2	6	6
		ow8a-89	319.39	AFB2	161	165
		ow8b-89	328.84	AFB2	6	6
		ow10a-89	319.68	AFB2	161	165
		ow10b-89	332.57	AFB2	6	6
	ASR	ow1-08	322.22	AFB2	161	165
		ow1a-02	325.84	AFB2	161	165
		ow1b-02	368.88	AFB1	1	3
		ow1a-96	185.82	Bedrock	5	0
		ow1c-96	289.01	AFC1	3	3
		ow1d-96	325.62	AFB2	161	165
		ow2a-02	319.77	AFB2	161	165
		ow2a-96	220.54	Bedrock	6	6
		ow2b-02	365.87	AFB1	4	3
		ow2b-96	326.82	AFB2	161	165
		ow3-09	324.01	AFB2	161	165
		ow3a-02	325.27	AFB2	161	165
		ow3b-02	367.75	AFB1	1	2
		ow4-09	317.01	AFB2	161	165
		ow4a-96	316.18	AFB2	6	6
		ow4b-96	329.93	AFB2	6	6
		ow5-02	334.56	AFB2	161	165
Total					4985	5085

5. Description of groundwater models

The groundwater flow model has a simulation domain of 5000 m × 5000 m in X- (East) and Y- (North) directions with the base elevation set as 200 masl and the top boundary as the topography. Prior to constructing the 3D groundwater flow model, a 2D grid was generated based on the plan view of the simulation domain, as shown in Figure 4 (a). Triangular elements with a size of 200 m were applied to discretize the simulation domain. At locations where there are water-supply and monitoring wells, the grid is refined by a factor of five.

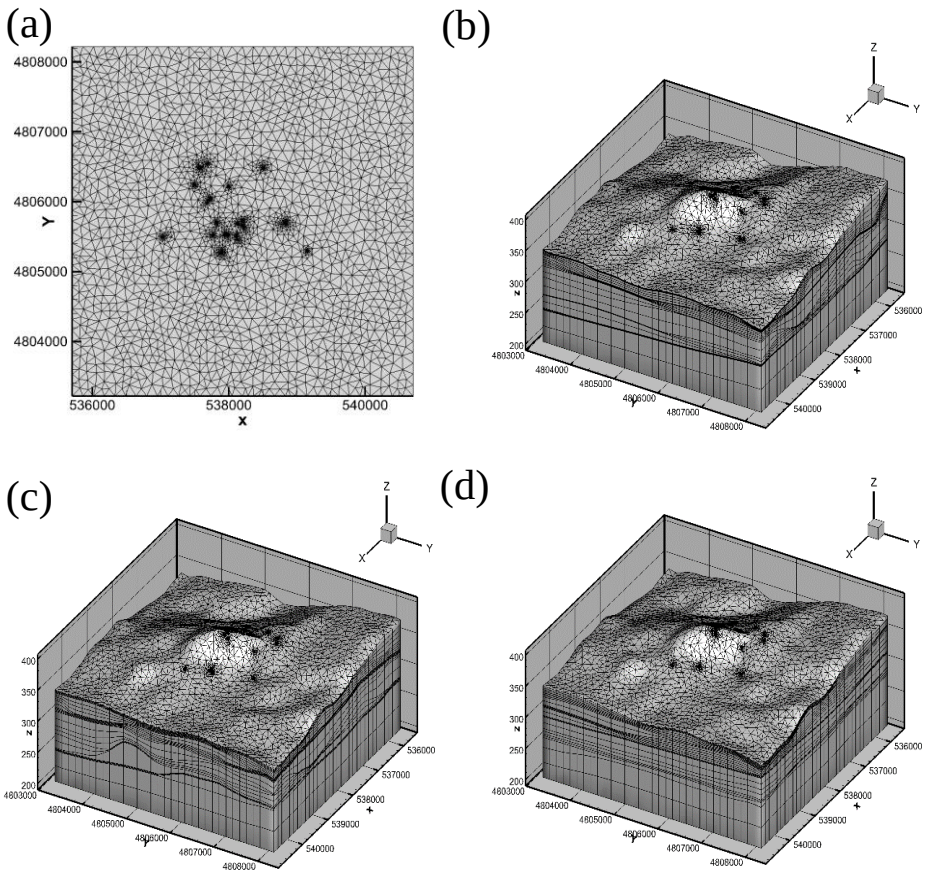

Fig. 4 (a) Generated two- dimensional grid of the study area (plan view). Generated three-dimensional grid for (b) 11-layer geological model, (c) the Waterloo model and (d) the Regional model.

Layer information identified in the constructed geological model was then introduced to generate the 3D groundwater flow model, as shown in Figure 4 (b), (c) and (d) for each geological model. Each geological layer is subdivided into several layers based on the approximate thickness as well as the distance to the pumping wells. In particular, fine grids are assigned to the layer of the water-supply aquifer, while coarse grids are assigned in upper and lower layers. In total, the 3D hydrogeologic model is discretized into 30 layers for both 5- and 11-layer geological models with 188,460 computational elements and 99,510 nodes, 27 layers for the Waterloo model with 144,482 elements and 76,842 nodes, and 27 layers for the Regional model with 139,412 elements and 74196 nodes. All four geological models were discretized using the same grid with uniform and isotropic *K* values of the elements located in the same layer.

All groundwater flow simulations are conducted using the groundwater flow and transport simulator HydroGeoSphere (HGS) (Aquanty Inc.) coupled with the parameter estimation code PEST (Doherty, 2005). In Case 1 (the Five-layer uni model), the initial *K* value for calibrating the 5-layer geological model was set as 6.00×10^{-5} m/s with a minimum bound of 1.00×10^{-9} m/day and a maximum bound of 0.01 m/day. The initial S_s value was set as 0.0006 m^{-1} with a minimum bound of 1.0×10^{-8} m^{-1} and a maximum bound of 0.1 m^{-1}. Since most observation points are located in AFB2, it is essential to set appropriate initial *K* and S_S values for the other layers in order to increase the computational efficiency and reliability of results. In particular, the predominant materials for each layer are identified and used to assign initial *K* and S_S

values, as shown in Table 2. The corresponding K and S_S values for each material are based on Martin and Frind (1998), provided in Appendix A. The representative values were identified by Martin and Frind (1998) from the literature and also calibrated based on previous pumping and slug tests results at the same wellfield site. Since there are several water-supply wells located within the ATB3 unit of the Waterloo model, and in order to increase the computational efficiency, the initial K and S_S values are set the same as AFB2 of the Waterloo model.

Four geological models with appropriate initial K and S_S values for each layer were calibrated and validated as Case 2, 3, 4 and 5. The minimum and maximum bounds of the estimated parameters in Case 2, 3, 4, 5 are set the same as in Case 1.

In terms of boundary conditions, the bottom face is defined as a no-flow boundary, since the bottom layer of all four models is Bedrock, which underlies the aquitard layer ATG1 for both 11-layer geological model and the Waterloo model. The four side faces are set as constant head boundaries, which implies that the hydraulic head on the boundary faces are not affected by pumping/injection events.

The static water level in the monitoring boreholes at the beginning of pumping records from 284 wells (mainly located at AFB2) within the area where each boundary of the area is 1 km larger than the study area is selected and used for kriging of hydraulic head with Tecplot. The resulting hydraulic heads are generally higher at the northwest part of the study area and lower at the southeast part of the study area, indicating that groundwater flows from the northeast to southwest, which is consistent with historical records.

The hydraulic head ranges from 306.28 masl to 359.25 masl within the study area and are used as initial head values for the simulation domain and constant boundary head for four boundary faces. It is noted that the hydraulic heads along the vertical direction on the side boundaries are set to be the same since there is no available hydraulic head data for lower aquifers in the study area.

In order to set the boundary condition for the top of the simulation domain, daily precipitation data from 2013 are obtained from the weather station located on the University of Waterloo campus. These data are modified as net precipitation (45% of the total precipitation for each day) and used as nodal fluxes to define the boundary condition at the top face. It is assumed that the effect of evapotranspiration (ET) is constant through the simulation period (six month). Guo (2017) studied the relationship between precipitation and ET in the year of 2010, 2011, 2012 and 2014 in the Laurel Creek Watershed, and found that the average simulated and measured annual ET accounted for 56.5% and 54.3% of the annual rainfall, respectively. Thus, 45% of the total precipitation is used as the net precipitation for each day during the simulation period. Since AFB1, which is hydraulically connected with AFB2, can directly receive recharge from precipitation, so the upper aquifer system could be affected by the rainfall.

Table 2. Nomenclature of geological, hydrogeologic units, and initial K and S_S values assigned to each layer of four geological models.

	Layer	Predominant Materials	Interpreted OGS Units	Initial K (m/s)	Initial S_S (/m)
5-layer Geological Model	AT1	Silty to clayey till	Upper Maryhill Till Port Stanley Till	5.00×10^{-10}	1.92×10^{-3}
	AF1	Mainly fine sand, some gravel	Upper/Middle Waterloo Moraine stratified sediments and equivalents Middle Marryhill Till and equivalents	5.00×10^{-4}	1.66×10^{-4}
	AT2	Silty to clayey till	Lower Maryhill Till Upper/Main Catfish Creek Till	5.00×10^{-10}	1.92×10^{-3}
	AF2	Sand and gravel	Catfish stratified deposits Canning Drift (pre- Catfish Creek Till)	1.00×10^{-3}	7.60×10^{-5}
	AT3	Limestone, dolostone, shale	Pre- Canning coarse- textured glaciofluvial/ glaciolacustrine seds Pre- Canning coarse- textured till Guelph, Salina, Bass islands, Bois Blanc Fm	1.00×10^{-8}	3.28×10^{-6}
11- layer Geological Model	ATB1	Silty to clayey till	Upper Maryhill Till Port Stanley Till	5.00×10^{-10}	1.92×10^{-3}
	AFB1	Mainly fine sand, some gravel	Upper Waterloo Moraine stratified sediments and equivalents	5.00×10^{-4}	1.66×10^{-4}
	ATB2	Silty to clayey till, silt, clay	Middle Marryhill Till and equivalents	5.00×10^{-10}	1.92×10^{-3}
	AFB2	Mainly fine sand, some gravel	Middle Waterloo Moraine stratified sediments and equivalents	5.00×10^{-4}	1.66×10^{-4}
	ATB3	Silty to clayey till	Lower Maryhill Till	5.00×10^{-10}	1.92×10^{-3}
	ATC1	Stony, silty to sandy till	Upper/Main Catfish Creek Till	1.00×10^{-7}	1.10×10^{-3}
	AFC1	Sand and gravel	Catfish stratified deposits	1.00×10^{-3}	7.60×10^{-5}
	ATE1	Silty to clayey till, silt, clay	Canning Drift (pre- Catfish Creek Till)	5.00×10^{-10}	1.92×10^{-3}
	AFF1	Sand and gravel	Pre- Canning coarse- textured glaciofluvial/ glaciolacustrine seds	1.00×10^{-3}	7.60×10^{-5}
	ATG1	Stony, silty to sandy till	Pre- Canning coarse- textured till	1.00×10^{-7}	1.10×10^{-3}
	Bedrock	Limestone, dolostone, shale	Guelph, Salina, Bass islands, Bois Blanc Fm	1.00×10^{-8}	3.28×10^{-6}
Waterloo Model	ATB1	Silty to clayey till	Upper Maryhill Till Port Stanley Till	5.00×10^{-10}	1.92×10^{-3}
	AFB1	Mainly fine sand, some gravel	Upper Waterloo Moraine stratified sediments and equivalents	5.00×10^{-4}	1.66×10^{-4}
	ATB2	Silty to clayey till, silt, clay	Middle Marryhill Till and equivalents	5.00×10^{-10}	1.92×10^{-3}
	AFB2	Mainly fine sand, some gravel	Middle Waterloo Moraine stratified sediments and equivalents	5.00×10^{-4}	1.66×10^{-4}
	ATB3	Silty to clayey till	Lower Maryhill Till	5.00×10^{-4}	1.66×10^{-4}
	ATC1	Stony, silty to sandy till	Upper/Main Catfish Creek Till	1.00×10^{-7}	1.10×10^{-3}
	AFD1	Sand and gravel	Pre- Catfish Creek sand and gravel	1.00×10^{-3}	7.60×10^{-5}
	ATE1	Silty to clayey till, silt, clay	Canning Drift (pre- Catfish Creek Till)	5.00×10^{-10}	1.92×10^{-3}
	AFF1	Sand and gravel	Pre- Canning coarse- textured glaciofluvial/ glaciolacustrine seds	1.00×10^{-3}	7.60×10^{-5}
	ATG1	Stony, silty to sandy till	Pre- Canning coarse- textured till	1.00×10^{-7}	1.10×10^{-3}
	Bedrock	Limestone, dolostone, shale	Guelph, Salina, Bass islands, Bois Blanc Fm	1.00×10^{-8}	3.28×10^{-6}
Regional Model	ATB1	Silty to clayey till	Upper Maryhill Till Port Stanley Till	5.00×10^{-10}	1.92×10^{-3}
	AFB1	Mainly fine sand, some gravel	Upper Waterloo Moraine stratified sediments and equivalents	5.00×10^{-4}	1.66×10^{-4}
	ATB2	Silty to clayey till, silt, clay	Middle Marryhill Till and equivalents	5.00×10^{-10}	1.92×10^{-3}
	AFB2	Mainly fine sand, some gravel	Middle Waterloo Moraine stratified sediments and equivalents	5.00×10^{-4}	1.66×10^{-4}
	ATB3	Silty to clayey till	Lower Maryhill Till	5.00×10^{-10}	1.92×10^{-3}
	AFB3	Layered gravel, sand or silt	Lower Waterloo Moraine stratified sediments or Catfish Creek outwash	1.00×10^{-3}	7.60×10^{-5}
	ATC1	Stony, silty to sandy till	Upper/Main Catfish Creek Till	1.00×10^{-7}	1.10×10^{-3}
	AFD1	Sand and gravel	Pre- Catfish Creek sand and gravel	1.00×10^{-3}	7.60×10^{-5}
	ATE1	Silty to clayey till, silt, clay	Canning Drift (pre- Catfish Creek Till)	5.00×10^{-10}	1.92×10^{-3}
	AFF1	Sand and gravel	Pre- Canning coarse- textured glaciofluvial/ glaciolacustrine seds	1.00×10^{-3}	7.60×10^{-5}
	Bedrock	Limestone, dolostone, shale	Guelph, Salina, Bass islands, Bois Blanc Fm	1.00×10^{-8}	3.28×10^{-6}

Refined hydrostratigraphic units are defined by Terraqua Investigations Inc. (1995). Ontario Geological Survey (OGS) units are defined by the work

6. Results and discussion

6.1. Model calibration results

Inverse modeling of pumping/injection records from 13 well-supply wells were performed on the same PC with a six-core CPU and 16 GB of Random Access Memory for model calibration. Calibration of the 5-layer geological model took about 24 hours to estimate 10 unknowns within 361 model calls for Case 1 and 2, while the calibration of other three geological models were all completed within 72 hours to estimated 22 unknowns with total model calls ranging from 627 for the Regional model (Case 5) to 849 for the 11-layer geological model (Case 3).

The estimated K and S_S distributions are plotted in Figure 5 and Figure 6 as a set of K and S_S is estimated for each layer in all models. The estimated K and S_S values and their 95% confidence intervals are summarized in Table 3.

The estimated K and S_S values in Case 1 are less realistic compared with the ones for the same geological layer in other cases. Their corresponding 95% confidence intervals are extremely large, especially for the lower geological layers. The extremely large 95% confidence intervals may be due to the merging layers of different K values and also a result of insufficient observation points, which have been suggested by Zhao and Illman (2018) in relation to a different site.

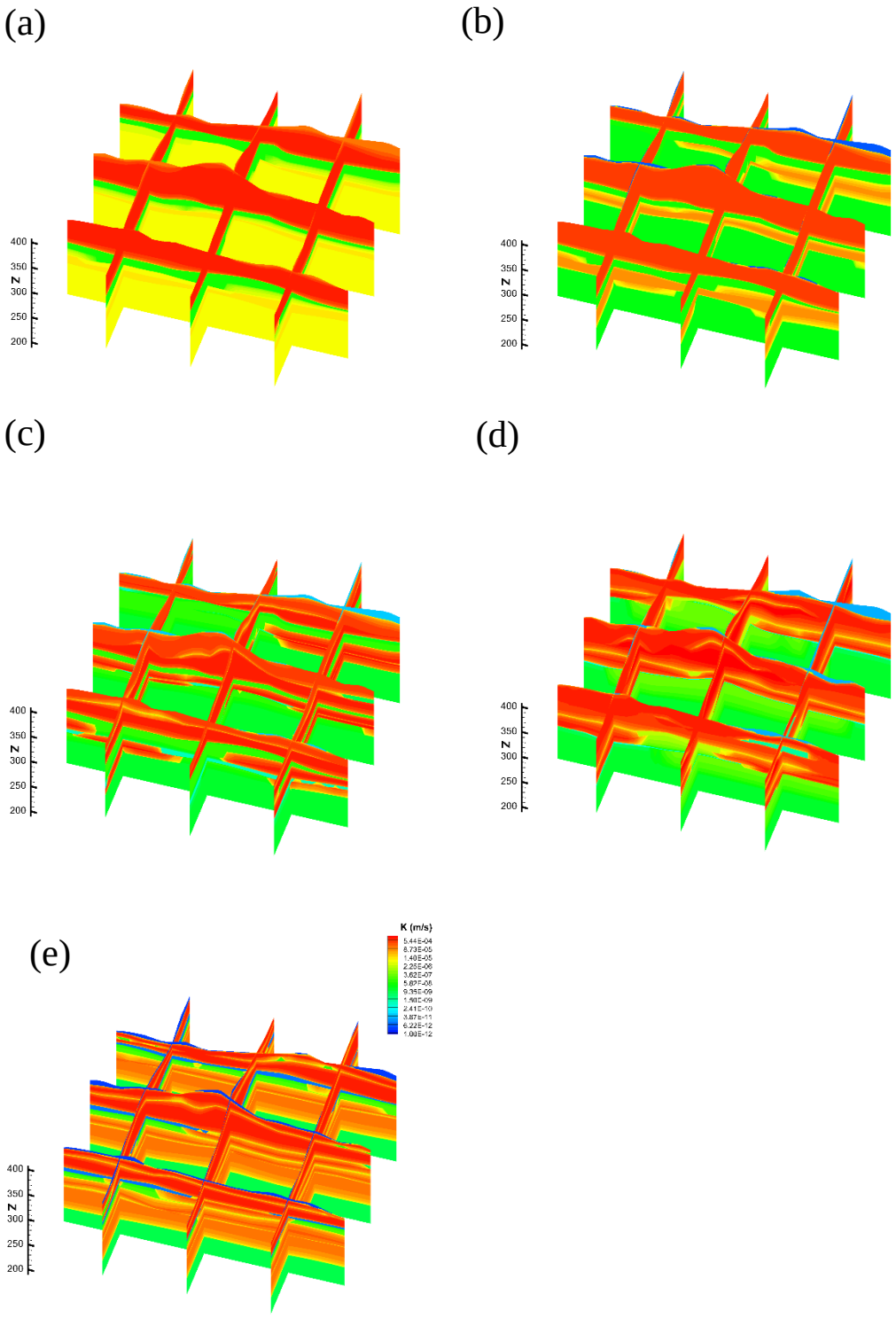

Fig. 5 Estimated K fields from the inversion of pumping and injection events by 13 water-supply wells during January to June, 2013 for: (a) the 5-layer uni model; (b) the 5-layer geological model; (c) the 11-layer geological model; (d) the Waterloo model; and (e) the Regional model.

Four geological models with appropriate initial K and S_S values (Case 2, 3,4 and 5) are all well calibrated with more realistic estimations and much smaller 95% confidence intervals compared with Case 1. Thus, the reliability of estimated hydraulic parameters can be greatly increased by using appropriate initial K and S_S values as prior information. As previously noted, most data points are collected from the water-monitoring boreholes located at the bottom of AFB2, so similar K and S_S values were obtained from model calibration for the11-layer geological model (Case 3) and the Regional model (Case 5). The K estimated for AFB2 is 8.14×10^{-4} m/s with the 11-layer geological model (Case 3) while a value of 5.17×10^{-4} m/s is estimated for the 5-layer geological model (Case 2), which is a consequence of using one layer to represent multiple soil types. The estimated K of AFB2, ATB3 and ATC1 for the Waterloo model (Case 4) is relatively large (1.21×10^{-3}m/s), which may due to the inaccurate classification of geological layer. Since most of the screens are located at AFB2 and ATB3, the large value of K of the aquitard enable the groundwater to be pumped from it and match the corresponding observed drawdowns at monitoring wells. Golder Associates Ltd (2011) summarized the K values at each water-supply well (Appendix B), ranging from 9×10^{-4} m/s to 1×10^{-1} m/s from well to well, which is similar with the estimated K values for AFB2 in this study.

The 95% confidence intervals for the estimated K for the upper part of the domain including ATB1, AFB1, ATB2, AFB2, ATB3, ATC1, are relatively small in Case 2, 3, 4 and 5, even with inaccurate layer information. The lower aquifer layer of the 5-layer geological model is constructed by combining AFC1, ATE1 and AFF1 and assigning

the initial K based on the property of two aquifers, but in reality, AFC1 and ATE1 are two discontinuous shallow aquifers with thicker aquitard ATE1 lying between these two aquifers. Such a merged layer would affect the reliability of the K estimate which is evident through the extremely large 95% confidence intervals.

The estimated S_S values results are similar to K in that more reliable results are obtained at the shallow region of the system and large confidence intervals are mainly concentrated for the lower layers of the 5-layer uni model and 5-layer geological model (Case 1 and 2) and the Waterloo models (Case 4). The estimated S_S values are found to vary in the range of 3.32×10^{-6}/m to 1.95×10^{-3} /m for the 11-layer geological model (Case 3), while for the 5-layer geological model (Case 2), S_S varies between 3.32×10^{-6}/m to 1.95×10^{-3} /m. The S_S values estimated for AFB2 varies from 8.35×10^{-5}/m for the Waterloo model to 3.16×10^{-4} /m for the Regional model. Compared with previous estimates of S by Luo and Illman (2016) which ranged from 0.002 to 0.736 with the thickness of AFB2 from 12 to 40 m within the same domain, the range is greatly reduced and the values are much smaller. S values estimated from previous aquifer tests for individual wells varies from 0.006 to 0.22 at the same study site (Trow Dames and Moore, 1990; CH2M and Papadopulos Associates; 2003CH2M HILL, 2003), which are consistent with those estimated through this study.

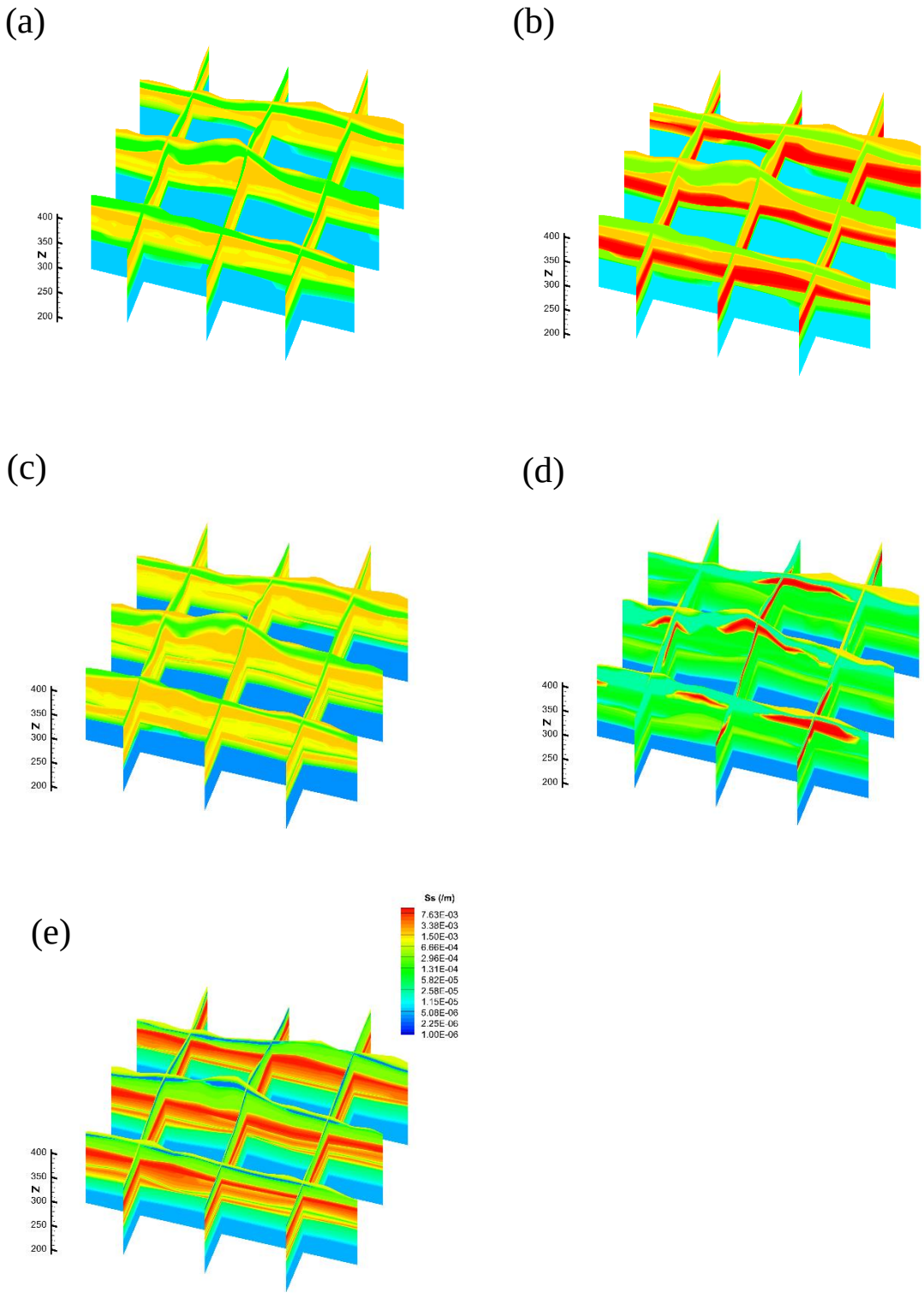

Fig. 6 Estimated S_S fields from the inversion of pumping and injection events by 13 water-supply wells during January to June, 2013 for: (a) the 5-layer uni model; (b) the 5-layer geological model; (c) the 11-layer geological model; (d) the Waterloo model; and (e) the Regional model.

Table 3. Estimated K and S_S values as well as their posterior 95% confidence intervals for five cases.

	Layer	Estimated K (m/s)	95% Confidence intervals		Estimated S_S (/m)	95% Confidence intervals	
			Upper limit	Lower limit		Upper limit	Lower limit
Case 1: 5-layer Uni	AT1	9.25×10^{-5}	7.45×10^{-13}	1.15×10^{4}	1.30×10^{-2}	2.97×10^{-5}	5.66
	AF1	6.60×10^{-4}	4.00×10^{-4}	1.01×10^{-3}	3.67×10^{-4}	1.16×10^{-5}	116×10^{-2}
	AT2	3.60×10^{-8}	8.31×10^{-10}	1.56	7.49×10^{-3}	1.34×10^{-22}	4.18×10^{13}
	AF2	7.64×10^{-6}	2.49×10^{-41}	2.85×10^{31}	3.57×10^{-4}	4.93×10^{-16}	2.58×10^{8}
	AT3	4.28×10^{-6}	1.97×10^{-16}	9.40×10^{5}	1.00×10^{-5}	2.35×10^{-43}	4.29×10^{32}
Case 2: 5- layer Geological Model	AT1	5.36×10^{-12}	1.73×10^{-12}	1.66×10^{-11}	1.81×10^{-3}	1.77×10^{-3}	1.86×10^{-3}
	AF1	5.17×10^{-4}	4.93×10^{-4}	5.41×10^{-4}	2.96×10^{-4}	1.00×10^{-4}	8.50×10^{-4}
	AT2	4.46×10^{-8}	3.09×10^{-8}	6.42×10^{-8}	1.46×10^{-2}	6.18×10^{-3}	3.43×10^{-2}
	AF2	7.53×10^{-5}	7.29×10^{-15}	7.78×10^{5}	3.73×10^{-4}	9.47×10^{-84}	1.47×10^{76}
	AT3	1.88×10^{-8}	1.86×10^{-8}	1.90×10^{-8}	6.78×10^{-6}	1.01×10^{-6}	4.56×10^{-5}
Case 3: 11- layer Geological Model	ATB1	4.09×10^{-11}	3.37×10^{-11}	4.98×10^{-11}	1.95×10^{-3}	1.95×10^{-3}	1.96×10^{-3}
	AFB1	3.84×10^{-4}	3.47×10^{-4}	4.24×10^{-4}	1.65×10^{-4}	1.65×10^{-4}	1.66×10^{-4}
	ATB2	7.28×10^{-9}	5.96×10^{-9}	8.89×10^{-9}	1.91×10^{-3}	1.90×10^{-3}	1.91×10^{-3}
	AFB2	8.14×10^{-4}	7.93×10^{-4}	8.37×10^{-4}	1.67×10^{-4}	1.66×10^{-4}	1.67×10^{-4}
	ATB3	5.03×10^{-10}	5.02×10^{-10}	5.04×10^{-10}	1.93×10^{-3}	1.92×10^{-3}	1.93×10^{-3}
	ATC1	1.00×10^{-7}	1.00×10^{-7}	1.00×10^{-7}	1.09×10^{-3}	1.09×10^{-3}	1.09×10^{-3}
	AFC1	9.94×10^{-4}	9.93×10^{-4}	9.96×10^{-4}	7.48×10^{-5}	7.46×10^{-5}	7.49×10^{-5}
	ATE1	4.99×10^{-10}	4.98×10^{-10}	5.00×10^{-10}	1.91×10^{-3}	1.91×10^{-3}	1.92×10^{-3}
	AFF1	1.02×10^{-3}	1.02×10^{-3}	1.02×10^{-3}	7.63×10^{-5}	7.62×10^{-5}	7.64×10^{-5}
	ATG1	9.91×10^{-8}	9.89×10^{-8}	9.93×10^{-8}	1.09×10^{-3}	1.09×10^{-3}	1.09×10^{-3}
	Bedrock	9.87×10^{-9}	9.85×10^{-9}	9.90×10^{-9}	3.32×10^{-6}	3.31×10^{-6}	3.33×10^{-6}
Case 4: Waterloo Model	ATB1	2.74×10^{-11}	7.90×10^{-24}	95.10	1.42×10^{-3}	3.17×10^{-16}	6.38×10^{93}
	AFB1	5.74×10^{-4}	4.23×10^{-4}	7.77×10^{-4}	2.16×10^{-5}	8.01×10^{-43}	5.80×10^{32}
	ATB2	1.37×10^{-9}	2.84×10^{-12}	6.65×10^{-7}	1.48×10^{-2}	7.03×10^{-3}	3.10×10^{-2}
	AFB2	1.21×10^{-3}	1.14×10^{-3}	1.28×10^{-3}	8.35×10^{-5}	1.03×10^{-10}	67.55
	ATB3	4.71×10^{-4}	3.50×10^{-4}	6.33×10^{-4}	6.66×10^{-5}	1.03×10^{-26}	4.31×10^{17}
	ATC1	2.12×10^{-6}	7.71×10^{-8}	5.82×10^{-5}	9.58×10^{-5}	5.41×10^{-15}	1.69×10^{6}
	AFD1	6.40×10^{-4}	7.56×10^{-14}	5.06×10^{5}	9.52×10^{-6}	8.61×10^{-17}	7.13×10^{7}
	ATE1	1.71×10^{-10}	8.32×10^{-23}	3.52×10^{2}	4.14×10^{-4}	4.20×10^{-15}	4.10×10^{7}
	AFF1	9.17×10^{-4}	8.15×10^{-12}	9.63×10^{5}	5.24×10^{-5}	6.58×10^{-12}	4.26×10^{5}
	ATG1	5.13×10^{-7}	4.22×10^{-25}	6.25×10^{11}	1.72×10^{-3}	5.38×10^{-23}	5.48×10^{14}
	Bedrock	1.52×10^{-8}	4.45×10^{-48}	5.22×10^{31}	2.96×10^{-6}	9.07×10^{-47}	9.67×10^{34}
Case 5: Regional Model	ATB1	1.96×10^{-12}	8.05×10^{-15}	4.76×10^{-10}	7.10×10^{-4}	6.25×10^{-4}	8.06×10^{-4}
	AFB1	7.24×10^{-4}	3.90×10^{-4}	1.35×10^{-3}	2.42×10^{-6}	1.55×10^{-6}	3.78×10^{-6}
	ATB2	6.25×10^{-8}	2.48×10^{-8}	1.58×10^{-7}	2.66×10^{-4}	2.51×10^{-4}	2.82×10^{-4}
	AFB2	8.62×10^{-4}	7.19×10^{-4}	1.02×10^{-3}	3.16×10^{-4}	2.98×10^{-4}	3.35×10^{-4}
	ATB3	7.89×10^{-12}	6.94×10^{-12}	8.96×10^{-12}	9.00×10^{-3}	8.85×10^{-3}	9.15×10^{-3}
	AFB3	4.38×10^{-4}	3.66×10^{-4}	5.25×10^{-4}	1.44×10^{-4}	1.33×10^{-4}	1.55×10^{-4}
	ATC1	1.57×10^{-7}	1.44×10^{-7}	1.71×10^{-7}	3.63×10^{-3}	3.57×10^{-3}	3.70×10^{-3}
	AFD1	1.85×10^{-4}	1.83×10^{-4}	1.86×10^{-4}	8.42×10^{-5}	7.69×10^{-5}	9.23×10^{-5}
	ATE1	4.76×10^{-10}	3.96×10^{-10}	5.71×10^{-10}	3.75×10^{-3}	3.42×10^{-3}	4.11×10^{-3}
	AFF1	3.18×10^{-4}	3.11×10^{-4}	3.26×10^{-4}	7.26×10^{-5}	7.18×10^{-5}	7.35×10^{-5}
	Bedrock	8.14×10^{-9}	7.62×10^{-9}	8.70×10^{-9}	4.34×10^{-6}	3.17×10^{-6}	5.95×10^{-6}

6.2. Performance of model calibrations

The performance of different geological conceptualizations on model calibration are evaluated by comparing the simulated drawdowns versus observed drawdowns from 28 observation locations used for model calibrations, as plotted in Figure 8. A linear model is fit for each geological model case for performance evaluation.

Generally, the fit greatly improves from Case 1 to Case 5, with the slopes of the linear model ranging from 0.76 to 1.15 and values of the coefficient of determination (R^2) increasing from 0.42 to 0.77. It is noted that the fit of the four geological models with appropriate initial K and S_S values (Case 2, 3, 4, 5) are quite similar with the slopes of the linear model ranging from 0.76 to 0.86 and values of R^2 increasing from 0.74 to 0.77. Although the estimated K and S_S are quite different in the four cases, the simulated drawdown can match the observed drawdown for all the four geological models quite well.

Quantitative assessment is conducted by computing the mean absolute error norm (L_1) and the mean square error norm (L_2). Those quantities are computed as:

(1) $$L_1 = \frac{1}{n}\sum_{i=1}^{n}|\chi_i - \widehat{\chi_i}|$$

(2) $$L_2 = \frac{1}{n}\sum_{i=1}^{n}(\chi_i - \widehat{\chi_i})^2$$

where *n* is the total number of drawdown data, i indicates the data number, χ_i and $\widehat{\chi_i}$ represent the estimates from simulated and measured drawdowns, respectively.

The calculated L_1 and L_2 values are shown on Figure 8. In particular, the calibration result based on the Regional model yields the smallest L_1 and L_2, while

the 5-layer uni model yields the largest L_1 and L_2. The L_1 and L_2 values for the 5-layer model and the 11-layer model (Case 3) are similar and this may be due to the similar hydraulic properties of AF1 and AFB2, where most of the observations are located.

Large errors are mainly observed at ow1-02 (Appendix C), where a rapid change in water levels is observed, but all the models fail to capture this fluctuation. In a previous study, Luo and Illman (2016) explained the lack of match as the potential existence of a high K pathway between some of the water-supply wells and water-monitoring boreholes.

HT based on geological models as presented in this study treats each geological layer as homogeneous and isotopic, but in reality, the aquifer layer is highly heterogeneous and could be anisotropic, thus a more sophisticated groundwater model that considers heterogeneity and anisotropy in each geological layer may be needed for future work to overcome this difficulty.

Another reason that may be contributing to the inconsistency is that the pumping/injection events normally operate for a couple of hours, but we use daily pumping/injection rates for each water-supply well, which could decrease the actual pumping/injection rate for the simulation process.

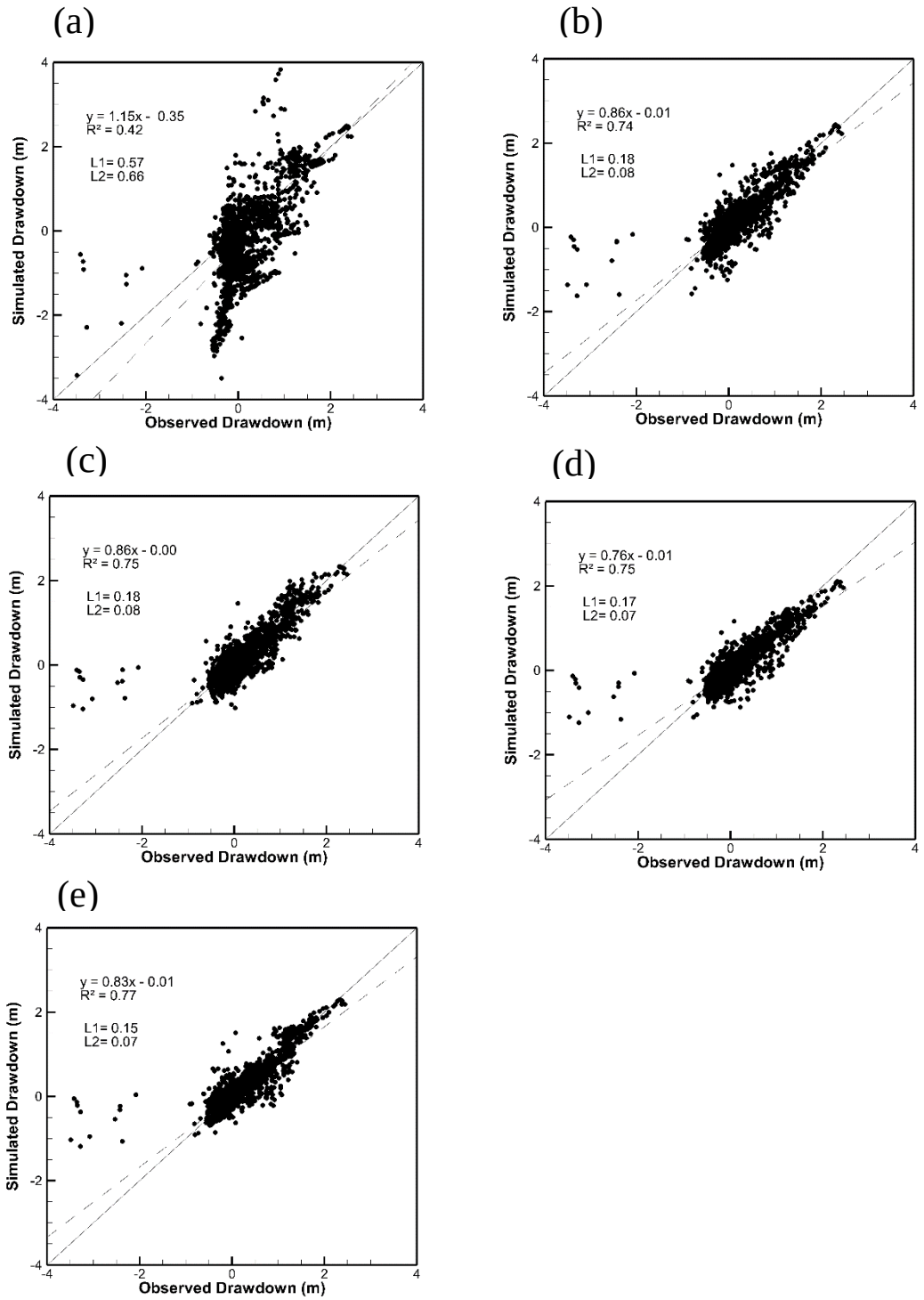

Fig. 7 Scatterplots of observed versus simulated drawdowns for model calibration based on 28 observation locations for: (a) the 5-layer uni model; (b) the 5-layer geological model; (c) the 11-layer geological model; (d) the Waterloo model; and (e) the Regional model. The solid line is a 1:1 line indicating a perfect match. The dash line is the best fit line. The linear fit results are also included on each plot.

6.3.Model validation results

The performance of different models in their abilities to predict drawdowns of monitoring wells are evaluated using the pumping/ injection record from July to December, 2013. The simulated drawdowns are compared with corresponding observed drawdowns to provide quantitative evaluation. Similar to the calibration results, the validation results for four geological models with appropriate initial K and S_S values (Case 2, 3, 4, 5) are similar in their overall shape in terms of the point distribution and the slope of the fit lines, while the 5-layer uni model in Case 1 yields the worst results with biased prediction. Since Case 2,3, 4 and 5 all capture the water level change and yield satisfactory result, the variability of evapotranspiration throughout the year may not be significant during the simulation period.

In a previous study, Zhao et al. (2016) found that as the number of pumping and monitoring points decreases, the performance gap among these approaches was reduced. Thus, the data set used in the calibration and validation processes may not be large enough to produce dramatic difference in the scatterplots among individual models. Although the slope of the linear model and R^2 for the 5-layer geological model are highest among the four models, it also yields relatively large L_1 and L_2 values. The 11-layer geological model and the Regional model both have the smallest L_1 and L_2, with a higher slope and a larger R^2 for the 11-layer geological model.

The simulated and observed drawdowns for each observation well are provided (see Appendix D), in which the5-layer uni model and the 5-layer geological model in Case 1 and 2 can better capture the rapid changes in water levels. The reason behind it

may be the higher K values for AT2 and merging AFB1, ATB2 and AFB2 into AF1 which create higher K pathways between the water-supply wells and observation boreholes.

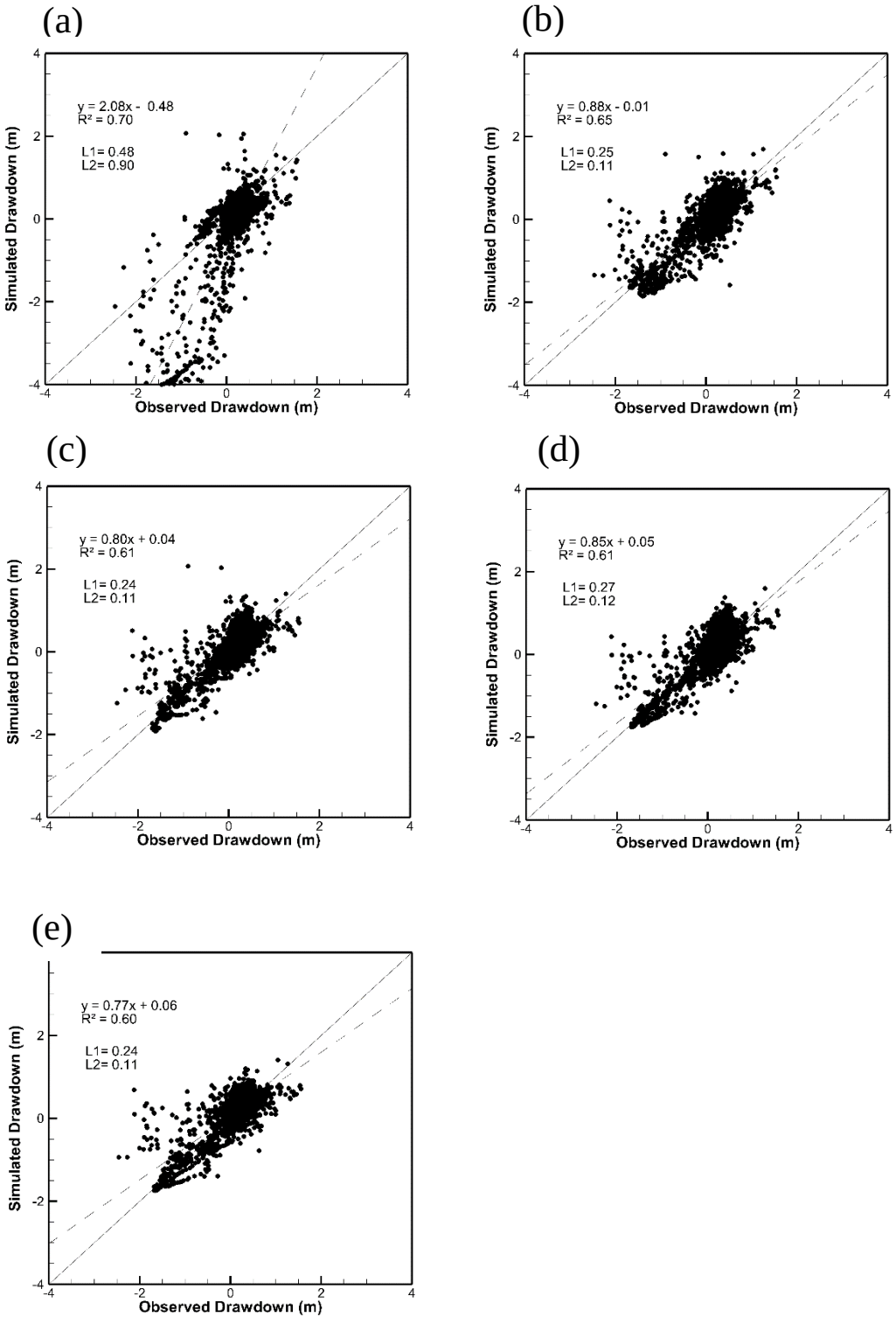

Fig. 8 Scatterplots of observed versus simulated drawdowns for model validation based on 28 observation locations for: (a) the 5-layer uni model; (b) the 5-layer geological model; (c) the 11-layer geological model; (d) the Waterloo model; and (e) the Regional model. The solid line is a 1:1 line indicating a perfect match. The dash line is the best fit line. The linear fit results are also included on each plot.

7. Summary and conclusions

In this study, we investigated the usefulness of hydraulic tomography (HT) analysis based on geological models at a municipal well field to estimate the spatial distribution of hydraulic parameters (i.e., K and S_S) using long term pumping/injection and monitoring well records. Pumping/injection rate data from 13 water-supply and water level data from 19 water- monitoring boreholes with 28 screens during the year of 2013 are selected and used for model calibration and validation. Four different geological conceptualizations with varying accuracy are used to examine the importance of geological data in HT analysis.

Our study resulted in the following findings and conclusions:

1. The calibration and validation both reveal that hydraulic parameters (i.e., K and S_S) can be estimated using long-term pumping/injection rates and corresponding water-level records from municipal well fields. The estimated parameters are compared with those estimated through independently conducted pumping tests. The hydraulic parameters from both studies are consistent.
2. Compared with traditional K and S_S estimation methods which are difficult to be conducted at well fields, the HT approach is successfully applied in this study through the use of long-term pumping/injection rates and corresponding water-level records. The use of such data for inverse modeling results in reliable hydraulic parameter estimates, while enhancing cost and time efficiency in terms of site characterization. Therefore, it is suggested that these data are collected and used in future studies.

3. Although good matches are obtained for both model calibration and validation, the rapid water-level variation are not fully captured by the model. It is essential to apply a more sophisticated inverse model which considers the heterogeneity of the geological layer to better predict the water-level change and to obtain more reliable hydraulic estimates.
4. The density of observation points can greatly affect the reliability of estimated hydraulic parameters. The large 95% confidence intervals and inconsistent parameter estimates for deeper geological layers promote the need for deeper well installation as well as hydraulic investigation. In addition, prior information of estimated parameter used in the model can reduce confidence interval widths.
5. Hydrogeological data is critical for geological model construction. In this study, we find that the geological model constructed with hydrogeological information yields the smallest error norms for both groundwater model calibration and validation, so hydrogeological data is essential for HT analysis based on geological models to yield reliable hydraulic parameters and better capture local heterogeneity.
6. The variability in evapotranspiration throughout the year is not considered in this study, but it will become very important for longer simulation periods. Since the upper aquifer of the study area is directly recharged through precipitation, it may be necessary to more rigorously consider evapotranspiration and other complexities (e.g., surface water/groundwater interaction, long-term decline of groundwater levels due to dewatering operations, etc.) that are not factored into the present study. If important processes are left out in the model used to estimate parameters, it is

conceivable that the estimated parameters will be affected. This importance topic will require additional studies in the future.

7. Finally, this study applied a new approach to estimate hydraulic parameters for a municipal well field using existing long-term pumping/injection rates and water-level monitoring records. A more sophisticated inverse model which considers each aquifer/aquitard units to be heterogeneous is currently being built for the study site. It is anticipated that improved parameter estimates will be obtained, which should result in more robust predictions of groundwater level variations due to municipal well operations. All of this should benefit well field management, contaminant transport predictions, as well as improve source water protection.

References

Alexander, M., Berg, S.J., Illman, W.A., 2011. Field study of hydrogeologic characterization methods in a heterogeneous aquifer. Ground Water 49, 365–382. https://doi.org/10.1111/j.1745-6584.2010.00729.x.

ARANZ Geo Limited, 2015. Leapfrog Hydro 2.2.3. 3D Geological Modelling Software.

Bajc, A.F., M. J. Newton., 2007. Mapping the subsurface of Waterloo region, Ontario, Canada: An improved framework of Quaternary geology for hydrogeological applications. Journal of Maps, 219–230.

Bajc, A.F., J. Shirota., 2007. Three-dimensional mapping of surficial deposits in the Regional Municipality of Waterloo, southwestern Ontario. Groundwater Resources Study 3. Sudbury, ON: Ontario Geological Survey.

Berg, S.J., Illman, W.A., 2011a. Capturing aquifer heterogeneity: comparison of approaches through controlled sandbox experiments. Water Resour. Res. 47, 1–17. https://doi.org/10.1029/2011WR010429.

Berg, S.J., Illman, W.A., 2011b. Three-dimensional transient hydraulic tomography in a highly heterogeneous glaciofluvial aquifer-aquitard system. Water Resour. Res. 47. https://doi.org/10.1029/2011WR010616.

Berg, S.J., Illman, W.A., 2013. Field study of subsurface heterogeneity with steady state hydraulic tomography. Ground Water 51, 29–40. https://doi.org/10.1111/j.1745-6584.2012.00914.x.

Berg, S.J., Illman, W.A., 2015. Comparison of hydraulic tomography with traditional methods at a highly heterogeneous site. Groundwater 53, 71–89. https://doi.org/10.1111/gwat.12159.

Blackport Hydrogeology Inc., 2012a. Tier Three Water Budget and Local Area Risk Assessment: River wells; Pompeii, Woolner and Forwell well fields characterization study. Report prepared for the Regional Municipality of Waterloo. Waterloo, ON: Blackport Hydrogeology Inc.

Blackport Hydrogeology Inc., 2012b. Tier Three Water Budget and Local Area Risk Assessment: Waterloo North, William Street and Lancaster well fields characterization study Report prepared for the Regional Municipality of Waterloo. Waterloo, ON: Blackport Hydrogeology Inc.

Blackport, R.F., L. Dorfman., 2014. Developing science-based policy for protecting the Waterloo Moraine Groundwater Resource. Canadian Water Resources Journal 39(2). http://doi.org/10.1080/07011784.2014.914803.

Bohling, G.C., Zhan, X., Butler, J.J., Zheng, L., 2002. Steady shape analysis of tomographic pumping tests for characterization of aquifer heterogeneities Water Resour. Res. 38. https://doi.org/10.1029/2001WR001176. 60-1-60–15.

Bouwer, H., Rice, R.C., 1976. A slug test for determining hydraulic conductivity of unconfined aquifers with completely or partially penetrating wells. Water resources research, 12(3), 423-428.

Callow, I.P., 1996. Optimizing aquifer production for multiple wellfield conditions in Kitchener, Ontario. M.Sc. Thesis, University of Waterloo.

Cardiff, M., Barrash, W., Kitanidis, P.K., 2013a. Hydraulic conductivity imaging from 3-D transient hydraulic tomography at several pumping/observation densities. Water Resour. Res. 49, 7311–7326. http://dx.doi.org/10.1002/wrcr.20519.

Cardiff, M., Bakhos, T., Kitanidis, P.K., Barrash, W., 2013b. Aquifer heterogeneity characterization with oscillatory pumping: sensitivity analysis and imaging potential. Water Resour. Res. 49, 5395–5410.

Chen, X.H., Goeke, J., Ayers, J., Summerside, S., 2003. Observation well network design for pumping tests in unconfined aquifers. Journal of American Water Resources Association 39 (1), 17–32.

Cooper, H.H., C.E. Jacob, 1946. A generalized graphical method for evaluating formation constants and summarizing well field history, Am. Geophys. Union Trans. 27, 526-534.

Cooper, H. H., J. D. Bredehoeft, I. S. Papadopulos, 1967. Response of a finite diameter well to an instantaneous charge of water. Water Resources Research 1, 263–269.

Dames T., Moore, 1990. Mannheim aquifer short-term water supply development: report prepared for the Region of Waterloo. Trow Dames and Moore, Mississauga, ON.

Farvolden R. N., J. P. Greenhouse, P. F. Karrow, P. E. Pehme, L. C. Ross., 1987. Ontario Geoscience Research Fund Grant 128, Subsurface Quaternary stratigraphy of Kitchener- Waterloo, using borehole geophysics. OFR5623. Sudbury, ON: Ontario Geological Survey.

Freeze, R.A., Cherry, J.A., 1979. Groundwater: Englewood Cliffs, NJ, Prentice-Hall, 604.

Frind, E. O., J. W. Molson, M. R. Sousa, P. J. Martin, 2014. Insights from four decades of model development on the Waterloo Moraine, a review. Canadian Water Resources Journal 39(2). https://doi.org/10.1080/07011784.2014.914799.

Golder Associates Ltd., 2011. Tier Three Water Budget and Local Area Risk Assessment: Mannheim well fields characterization. Report prepared for the Regional Municipalityof Waterloo. Mississauga, ON: Golder Associates Ltd.

Harp D.R., Vesselinov V.V., 2011. Identification of pumping influences in long-term water level fluctuations. Ground Water 49(12). http://doi.org/10.111/ j.17456584.2010.00725.x.

Hazen A. Discussion: dams on sand foundations. Trans Am Soc Civ Eng. 1911;73:199–203.

Hvorslev, M.J., 1951. Time Lag and Soil Permeability in Ground-Water Observations, Bull. No. 36, Waterways Exper. Sta. Corps of Engrs, U.S. Army, Vicksburg, Mississippi, 1-50.

Illman, W.A., Liu, X., Craig, A., 2007. Steady-state hydraulic tomography in a laboratory aquifer with deterministic heterogeneity: multi-method and multiscale validation of hydraulic conductivity tomograms. J. Hydrol. 341, 222–234. https://doi.org/10.1016/j.jhydrol.2007.05.011.

Illman, W.A., Craig, A.J., Liu, X., 2008. Practical issues in imaging hydraulic conductivity through hydraulic tomography. Ground Water 46, 120–132. https://doi.org/10.1111/j.1745-6584.2007.00374.x.

Illman, W.A., Liu, X., Takeuchi, S., Yeh, T.C.J., Ando, K., Saegusa, H., 2009. Hydraulic tomography in fractured granite: Mizunami Underground Research site, Japan. Water Resour. Res. 45, 1–18. https://doi.org/10.1029/2007WR006715.

Illman, W.A., Zhu, J., Craig, A.J., Yin, D., 2010a. Comparison of aquifer characterization approaches through steady state groundwater model validation: a controlled laboratory sandbox study. Water Resour. Res. 46, 1–18. https://doi.org/10.1029/2009WR007745.

Illman, W.A., Berg, S.J., Liu, X., Massi, A., 2010b. Hydraulic/partitioning tracer tomography for trichloroethene source zone characterization: small-scale sandbox experiments. Environ. Sci. Technol. 44 (22), 8609–8614. http://dx.doi.org/ 10.1021/es101654j.

Illman, W.A., Berg, S.J., Zhao, Z., 2015. Should hydraulic tomography data be interpreted using geostatistical inverse modeling? A laboratory sandbox investigation. Water Resour. Res. 51, 3219–3237. https://doi.org/10.1002/2014WR016552.

International Water Supply Ltd., 1973. Kitchener-Waterloo groundwater evaluation. Report to the Regional Municipality of Waterloo. Barrie, ON: International Water Supply Ltd.

Karrow, P. F., 1993. Quaternary geology of the Stratford- Conestogo area, southern Ontario. Report 283. Sudbury, ON: Ontario Geological Survey.

Kitanidis, P. K., VoMvoris, E. G.,1983. A geostatistical approach to the inverse problem in groundwater modeling (steady state) and one-dimensional simulations. Water resources research, 19(3), 677-690.

Kozeny, J., 1927. Uber Kapillare Leitung Des Wassers in Boden. Sitzungsber Akad. Wiss.Wien Math.Naturwiss.Kl., Abt.2a, 136:271–306 (in German).

Lake Erie Region Source Protection Committee., 2012. Grand River source protection area, Approved Assessment Report.

Luo, N., Illman, W. A., 2016. Automatic estimation of aquifer parameters using long-term water supply pumping and injection records. Hydrogeology Journal, 24(6), 1443-1461. https://doi.org/10.1007/s10040-016-1407-x.

Luo, N., Zhao, Z., Illman, W. A., Berg, S. J., 2017. Comparative study of transient hydraulic tomography with varying parameterizations and zonations: Laboratory sandbox investigation. Journal of Hydrology, 554, 758-779. https://doi.org/10.1016/ j.jhydrol.2017.09.045.

Martin, P. J., and E.O. Frind, 1998. Modelling methodology for a complex multi-aquifer system: The Waterloo Moraine. Ground Water 36(4), 679–690.

Mas-Pla, J., Jim Yeh, T. C., Williams, T. M., McCarthy, J. F.,1997. Analyses of slug tests and hydraulic conductivity variations in the near field of a two-well tracer experiment site. Groundwater, 35(3), 492-501.

Matrix Solutions Inc. and S.S. Papadopulos and Associates, 2014a. Region of Waterloo Tier Three Water Budget and Local Area Risk Assessment; Model Calibration and Water Budget Report. August, 2014.

Matrix Solutions Inc. and S.S. Papadopulos and Associates, 2014b. Region of Waterloo Tier Three Water Budget and Local Area Risk Assessment; Final Risk Assessment Report. September, 2014.

Mishra P, Vesselinov V.V., 2011. WELLS: multi-well variable-rate pumping-test analysis tool. https://gitlab.com/monty/wells. Accessed 7 Feb 2014.

Molson, J.W., P.J. Martin, E.O. Frind. 1995. WATFLOW Version 1.0: A Three-Dimensional Groundwater Flow Model, User's Guide. Waterloo, Ontario, Canada: Waterloo Centre for Groundwater Research.

Paloschi, G.V.R., 1993. Subsurface stratigraphy of the Waterloo Moraine. M.Sc. project, University of Waterloo.

Regional Municipality of Waterloo, 2014. Region of Waterloo: hydrogeology and source water—WRAS database design manual. Regional Municipality of Waterloo, Waterloo, ON.

Rehfeldt, K.R., Boggs, J.M., Gelhar, L.W., 1992. Field study of dispersion in a heterogeneous aquifer: 3. Geostatistical analysis of hydraulic conductivity. Water Resources Research, 28(12), 3309-3324.

Refsgaard, J.C., Christensen, S., Sonnenborg, T.O., Seifert, D., Højberg, A.L., Troldborg, L., 2012. Review of strategies for handling geological uncertainty in groundwater flow and transport modeling. Adv. Water Resour. 36, 36–50. http://dx.doi.org/10.1016/j.advwatres.2011.04.006.

Riva, M., Guadagnini, A., Neuman, S.P., Janetti, E.B., Malama, B., 2009. Inverse analysis of stochastic moment equations for transient flow in randomly heterogeneous media. Advances in water resources, 32(10), 1495-1507.

Rubin, Y., and Dagan, G., 1987. Stochastic identification of transmissivity and effective recharge in steady groundwater flow: 1. Theory. Water Resources Research, 23(7), 1185-1192.

Rudolph, D.L., 1985. A quasi 3-dimensional finite element model for steady-state analysis of multi-aquifer systems. M.Sc. Thesis, University of Waterloo.

Rudolph, D.L., E.A. Sudicky, 1990. Simulation of groundwater flow in complex multiaquifer systems: Performance of quasi three-dimensional technique in the steadystate case. Canadian Geotechnical Journal 27: 590–600.

Shepherd R.G., 1989. Correlations of permeability and Grain-size. Groundwater. 27(5):633–638. http://dx.doi.org/10.1111/j.1745-6584.1989.tb00476.x.

Sudicky, E.A., 1986. A natural gradient experiment on solute transport in a sand aquifer: Spatial variability of hydraulic conductivity and its role in the dispersion process. Water Resources Research, 22(13), 2069-2082.

Sudicky, E.A., Illman, W.A., Goltz, I.K., Adams, J. J., McLaren, R.G., 2010. Heterogeneity in hydraulic conductivity and its role on the macroscale transport of a solute plume: From measurements to a practical application of stochastic flow and transport theory. Water Resources Research, 46(1).

Stantec Consulting Ltd., 2009. Tier Three Water Budget and Local Area Risk Assessment: Strange Street well field characterization n study. Report prepared for the Regional Municipality of Waterloo. Kitchener, ON: Stantec Consulting Ltd.

Stantec Consulting Ltd., 2012a. Tier Three Water Budget and Local Area Risk Assessment: Erb Street well field characterization study. Report prepared for the Regional Municipality of Waterloo. Kitchener, ON: Stantec Consulting Ltd.

Stantec Consulting Ltd., 2012b. Tier Three Water Budget and Local Area Risk Assessment: Greenbrook well field characterization study. Report prepared for the Regional Municipality of Waterloo. Kitchener, ON: Stantec Consulting Ltd.

Stantec Consulting Ltd., 2012c. Tier Three Water Budget and Local Area Risk Assessment: Parkway and Strasburg well field characterization study. Report prepared for the Regional Municipality of Waterloo. Kitchener, ON: Stantec Consulting Ltd.

Terraqua Investigations Ltd., 1992. Waterloo north aquifer system study. Report prepared for the Regional Municipality of Waterloo. Waterloo, ON: Terraqua Investigations Ltd.

Terraqua Investigations Ltd., 1995. Study of the hydrogeology of the Waterloo Moraine. Report prepared for the Regional Municipality of Waterloo. Waterloo, ON: Terraqua Investigations Ltd.

Theis, C.V., 1935. The relation between the lowering of the piezometric surface and the rate and duration of discharge of a well using groundwater storage. Am. Geophys. Union Trans 16: 519-524.

Wu, C.M., Yeh, T.C.J., Zhu, J., Tim, H.L., Hsu, N.S., Chen, C.H., Sancho, A.F., 2005. Traditional analysis of aquifer tests: Comparing apples to oranges? Water Resour. Res. 41, 1–12. https://doi.org/10.1029/2004WR003717.

Yeh T. C.J., Lee C. H., 2007. Time to change the way we collect and analyze data for aquifer characterization. GroundWater 45(2):116–118. https://doi.org/10.1111/j.1745-6584.2006.00292.x.

Yeh, T.C.J., Liu, S., 2000. Hydraulic tomography: development of a new aquifer test method. Water Resour. Res. 36, 2095. https://doi.org/10.1029/2000WR900114.

Yeh, T.C.J., Jin, M., Hanna, S., 1996. An iterative stochastic inverse method: conditional effective transmissivity and hydraulic head fields. Water Resour. Res. 32, 85–92. https://doi.org/10.1029/95WR02869.

Zhao, Z., Illman, W.A., 2017. On the importance of geological data for threedimensional steady-state hydraulic tomography analysis at a highly heterogeneous aquifer-aquitard system. J. Hydrol. 544, 640–657. https://doi.org/10.1016/j.jhydrol.2016.12.004.

Zhao, Z., Illman, W.A., 2018. Three-dimensional imaging of aquifer and aquitard heterogeneity via transient hydraulic tomography at a highly heterogeneous field site. Journal of Hydrology, 559, 392-410. https://doi.org/10.1016/j.jhydrol.2018.02.024.

Zhao, Z., Illman, W.A., Berg, S.J., 2016. On the importance of geological data for hydraulic tomography analysis: laboratory sandbox study. J. Hydrol. 542, 156–171. https://doi.org/10.1016/j.jhydrol.2016.08.061.

Appendix

Appendix A. Hydraulic conductivity values for corresponding lithologic units (from:Martin and Frind, 1998).

Table 2
Standardized Lithologic Categories and Hydraulic Conductivities

Material Number	Lithologic Unit	Hydraulic Conductivity (m/s) From Literature*	From Field Measurements	Final Calibrated K_h	Final Calibrated K_v
2	Clay	$10^{-9} - 10^{-12}$	$2\times10^{-9} - 3\times10^{-11}$	1×10^{-11}	1×10^{-12}
3	Silty clay	$10^{-9} - 10^{-11}$	–	1×10^{-10}	1×10^{-11}
4	Sandy clay	$10^{-7} - 10^{-10}$	–	1×10^{-8}	1×10^{-9}
5	Gravelly clay	$10^{-7} - 10^{-9}$	$1\times10^{-7} - 1\times10^{-10}$	5×10^{-8}	5×10^{-9}
6	Clayey silt	$10^{-7} - 10^{-9}$	$3\times10^{-7} - 2\times10^{-8}$	1×10^{-9}	1×10^{-10}
7	Silt	$10^{-5} - 10^{-9}$	$1\times10^{-6} - 1\times10^{-10}$	5×10^{-8}	5×10^{-9}
8	Sandy silt	$10^{-6} - 10^{-8}$	$4\times10^{-7} - 2\times10^{-9}$	5×10^{-7}	5×10^{-8}
9	Gravelly silt	$10^{-5} - 10^{-7}$	$1\times10^{-6} - 1\times10^{-7}$	1×10^{-6}	1×10^{-7}
10	Clayey sand	$10^{-5} - 10^{-7}$	–	5×10^{-5}	5×10^{-6}
11	Silty sand	$10^{-1} - 10^{-5}$	$1\times10^{-6} - 1\times10^{-6}$	5×10^{-4}	5×10^{-5}
12	Fine sand	$10^{-4} - 10^{-6}$	$2\times10^{-4} - 3\times10^{-6}$	1×10^{-3}	1×10^{-4}
13	Medium sand	$10^{-2} - 10^{-6}$	$4\times10^{-4} - 4\times10^{-6}$	5×10^{-3}	1×10^{-3}
14	Coarse sand	$10^{-2} - 10^{-4}$	$5\times10^{-3} - 2\times10^{-6}$	1×10^{-2}	5×10^{-3}
15	Gravel	$10^{0} - 10^{-3}$	$2\times10^{-3} - 4\times10^{-4}$	5×10^{-2}	1×10^{-2}
16	Limestone bedrock	$10^{-2} - 10^{-9}$	–	1×10^{-4}	1×10^{-4}
17	Shale bedrock	$10^{-9} - 10^{-13}$	–	1×10^{-8}	1×10^{-8}
99	Unknown	–	–	1×10^{-4}	1×10^{-5}

*Freeze and Cherry 1979.

Appendix B. Hydraulic conductivity estimated from previous studies for individual well (from: Golder Associates Ltd, 2011).

Well	Saturated Thickness	Specific Capacity	Transmissivity[1]	Hydraulic Conductivity[2]	Maximum Pumping Rate
	(m)	(L/s per m drawdown)	m^2/day	(m/s)	(L/s)
ASR-1	16.0	8.8	5,292	4×10^{-3}	53.0
ASR-2	13.1	5.1	1,370	1×10^{-3}	37.9
ASR-3	12.8	8.8	2,118	2×10^{-3}	45.7
ASR-4	19.8	6.7	2,830	1×10^{-3}	63.1
RCW-1	12.5	6.2	3,023	3×10^{-3}	69.4
RCW-2	19.0	6.2	2,885	2×10^{-3}	63.1
K22A	16.0	6.9	1,700	1×10^{-1}	42.0
K25	14.0	34.3	5,550	4×10^{-1}	46.0
K26	21.0	9.9	13,600	7×10^{-1}	100.0
K91	18.8	5.5	2,277	8×10^{-4}	50.0
K92	17.2	21.5	1,318	1×10^{-3}	91.0
K93	18.0	10.6	1,976	1×10^{-3}	72.0
K94	19.7	8.7	1,581	9×10^{-4}	68.0

Notes: - values provided for ASR-1 through RCW-2 taken from Table 7.3 in the Stage 1 ASR Conceptual Design Report (CH2M Hill, 2003)
- values provided for K22A, K25 and K26 taken from Table 3.2 in the Hydrogeological Study to Evaluate the GUDI Status of the Mannheim West, Mannheim East and Peaking Well Fields (CH2M Hill, 2002)
- values provided for K91 through K94 taken from the Peaking Well Construction Program Report (Trow, Dames & Moore, 1990)
[1] - reported transmissivity for ASR-1 through RCW-2 reflects an average of interpreted tranmissivity estimates provided in Table 7.3 of Golder (2009)
[2] - reported hydraulic conductivity for ASR-1 through RCW-2 reflects a geometric mean of interpreted hydraulic conductivity estimates provided in Table 7.3 of Golder (2009)

Appendix C. Drawdown versus time for model calibration including measured drawdown, simulated drawdown for five cases.

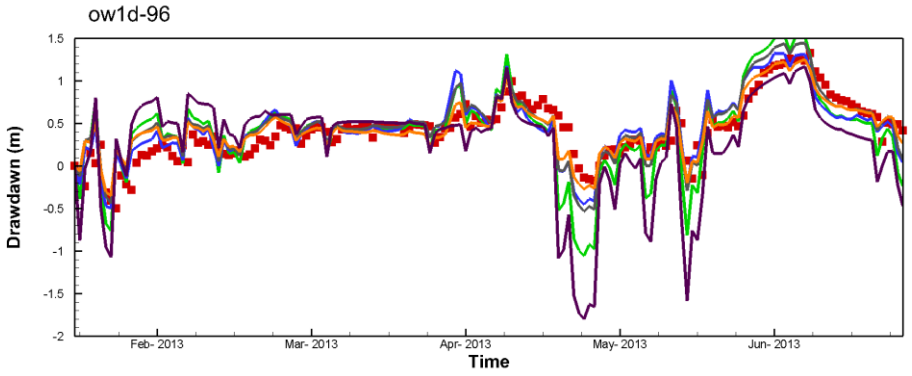

ow2a-96

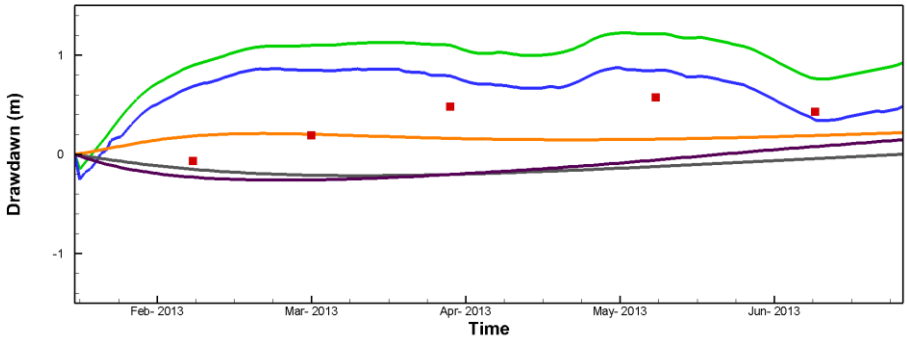

ow2b-02

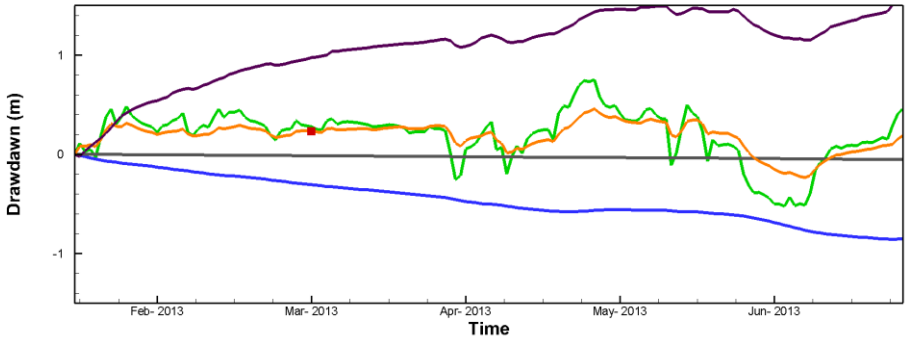

ow1c-96

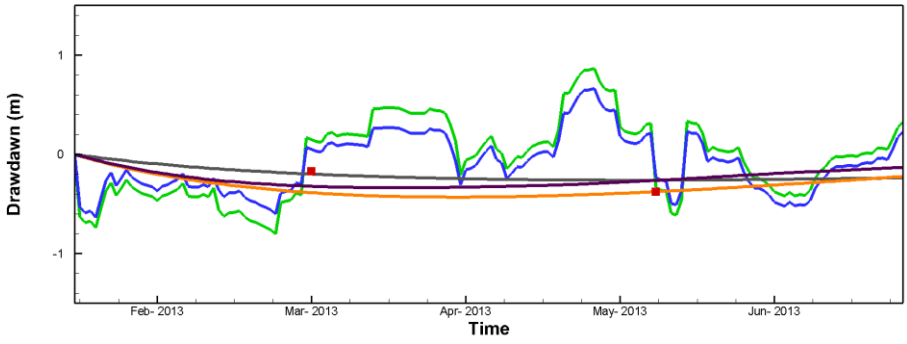

ow2b-96

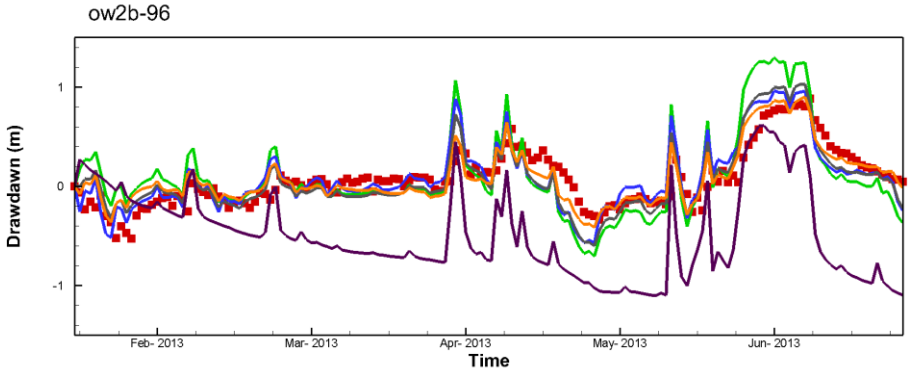

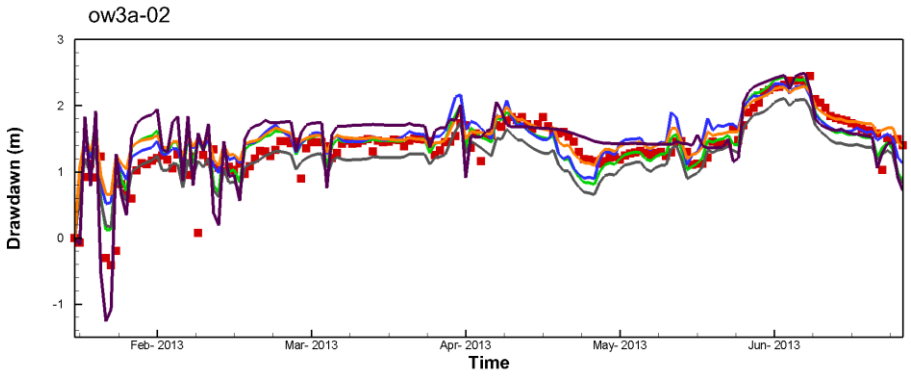
ow3a-02
Drawdawn (m)
3
2
1
0
-1
Feb- 2013
Mar- 2013
Apr- 2013
May- 2013
Jun- 2013
Time

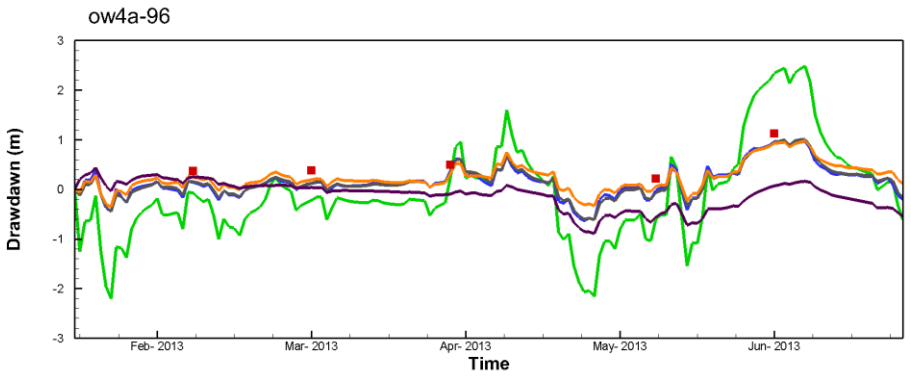
ow4a-96
Drawdawn (m)
3
2
1
0
-1
-2
-3
Feb- 2013
Mar- 2013
Apr- 2013
May- 2013
Jun- 2013
Time

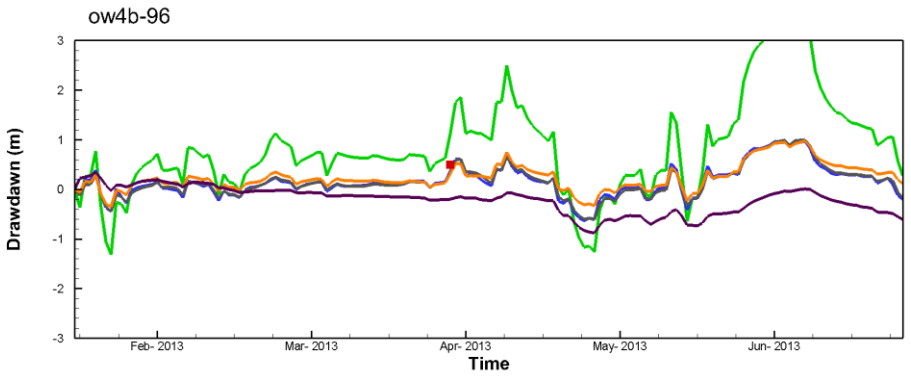
ow4b-96
Drawdawn (m)
3
2
1
0
-1
-2
-3
Feb- 2013
Mar- 2013
Apr- 2013
May- 2013
Jun- 2013
Time

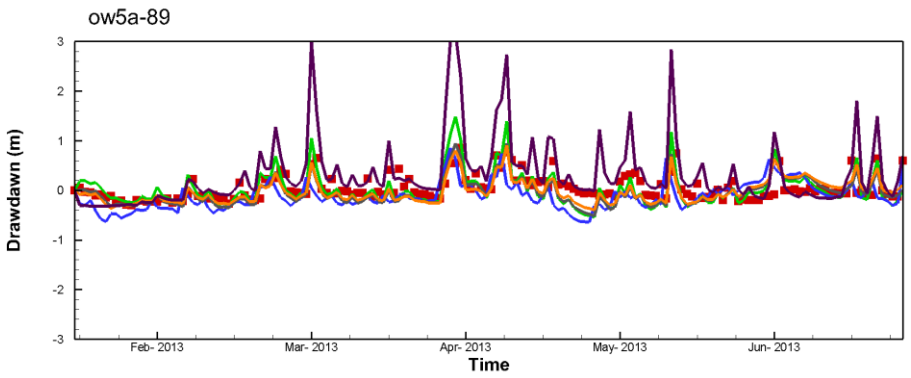
ow5a-89
Drawdawn (m)
3
2
1
0
-1
-2
-3
Feb- 2013
Mar- 2013
Apr- 2013
May- 2013
Jun- 2013
Time

ow8b-89

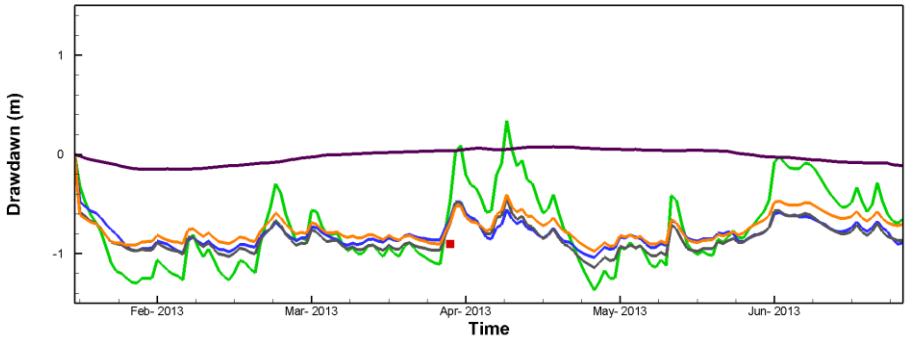

ow5b-89

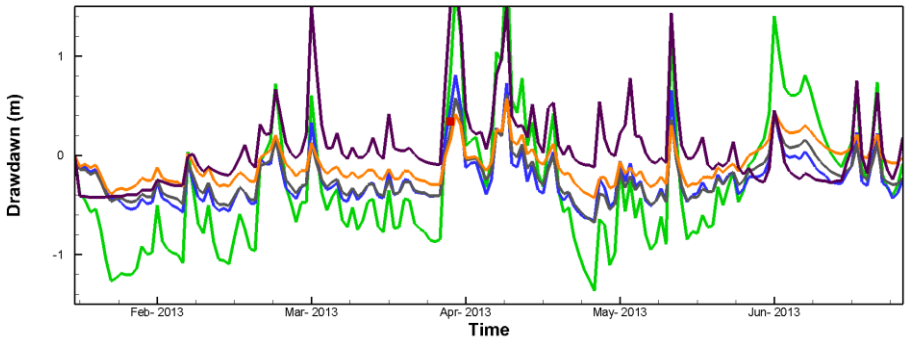

ow10b-89

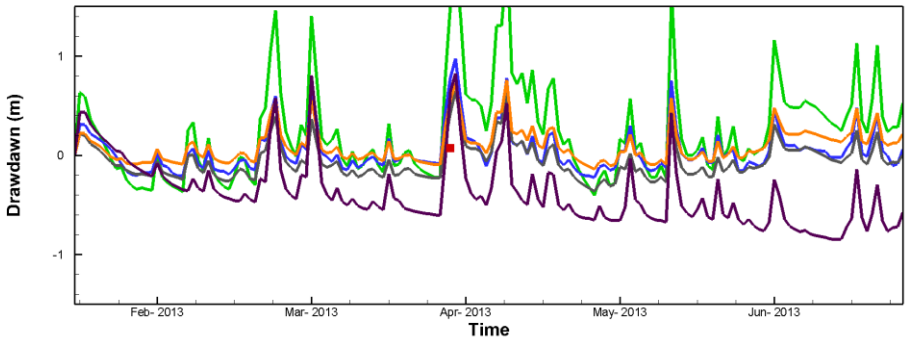

ow1-02

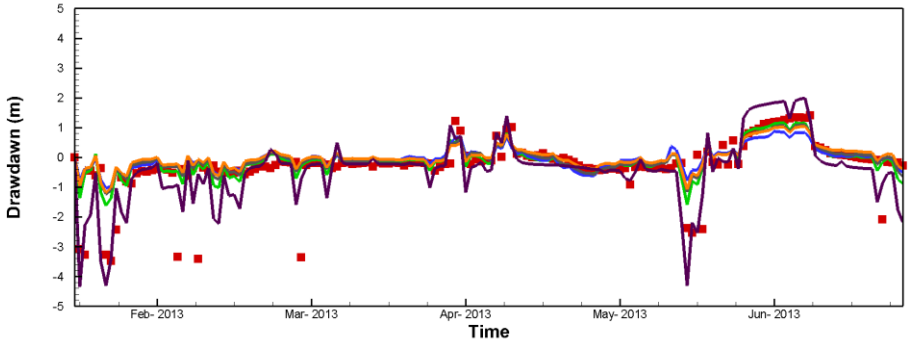

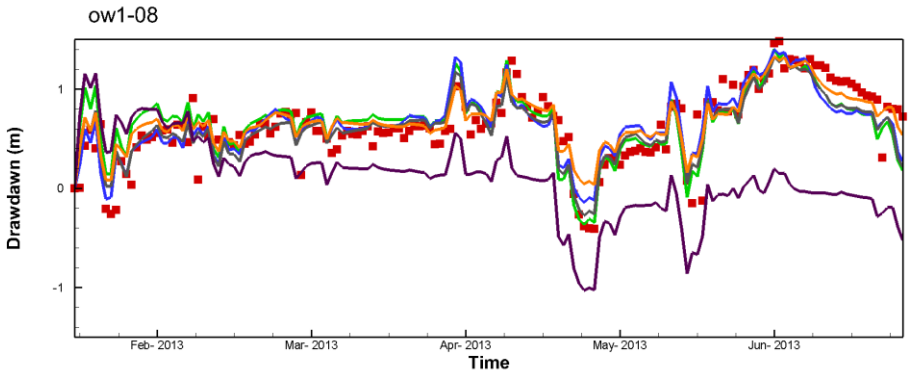
ow1-08
Drawdawn (m)
1
0
-1
Feb- 2013
Mar- 2013
Apr- 2013
May- 2013
Jun- 2013
Time

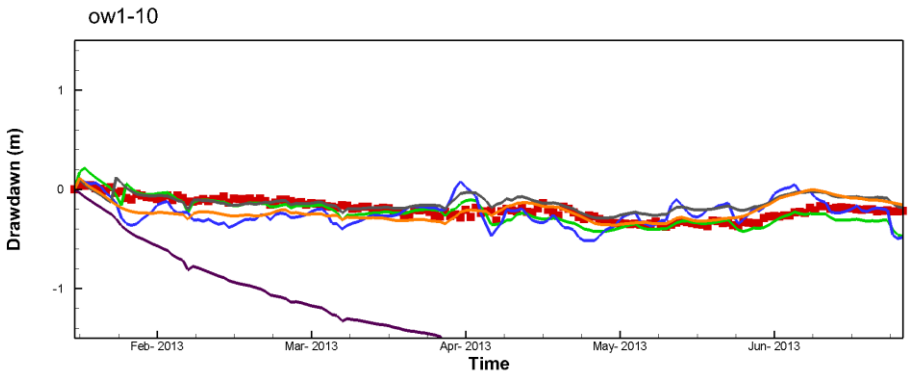
ow1-10
Drawdawn (m)
1
0
-1
Feb- 2013
Mar- 2013
Apr- 2013
May- 2013
Jun- 2013
Time

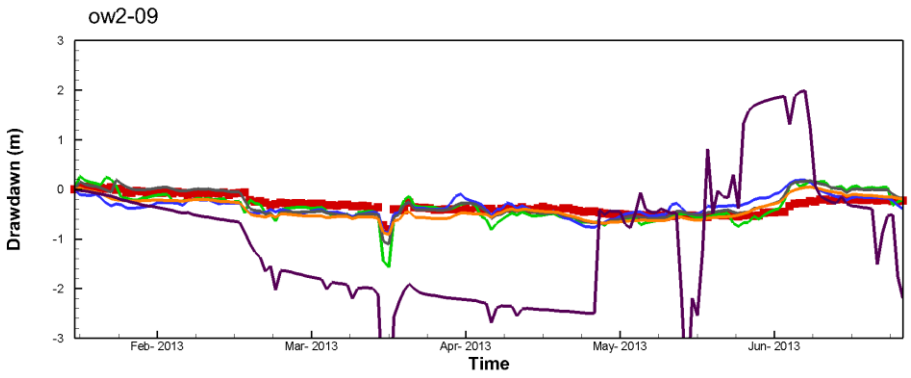
ow2-09
Drawdawn (m)
3
2
1
0
-1
-2
-3
Feb- 2013
Mar- 2013
Apr- 2013
May- 2013
Jun- 2013
Time

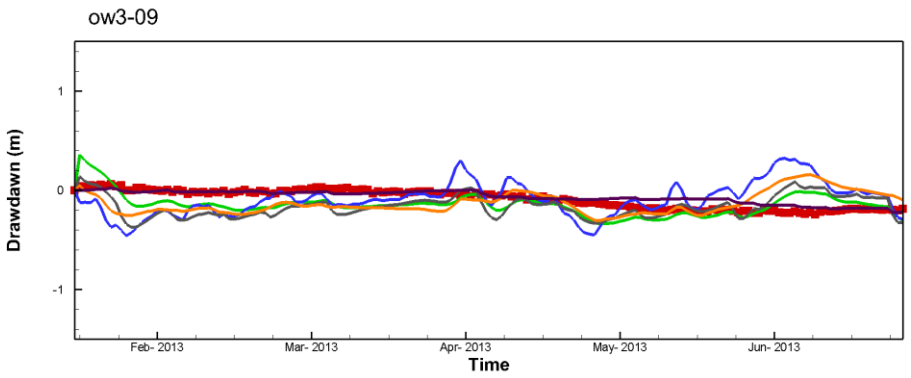
ow3-09
Drawdawn (m)
1
0
-1
Feb- 2013
Mar- 2013
Apr- 2013
May- 2013
Jun- 2013
Time

ow3-85

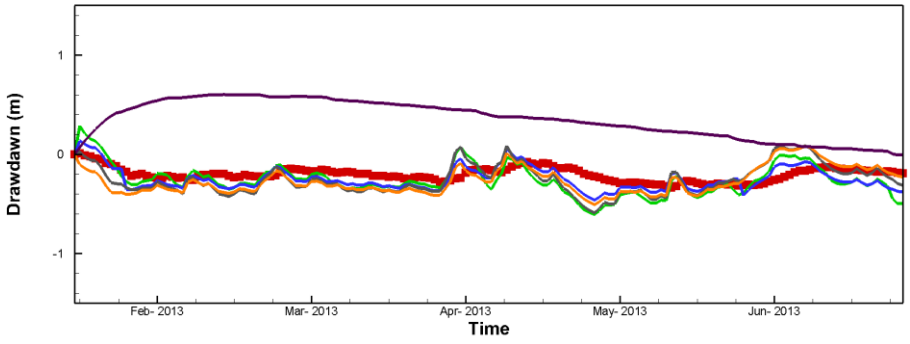

ow4-09

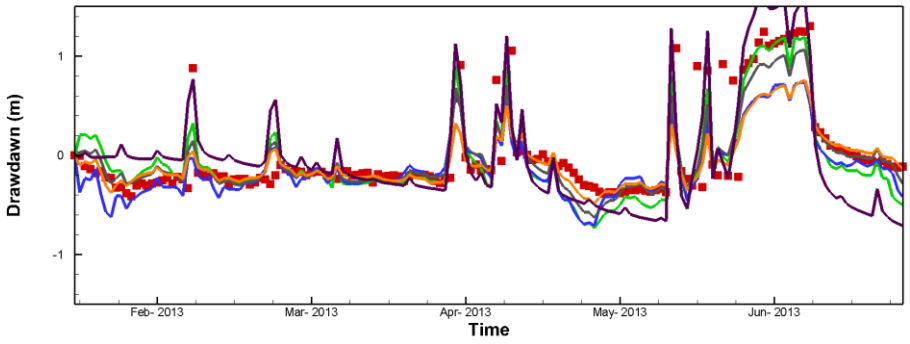

ow2a-02

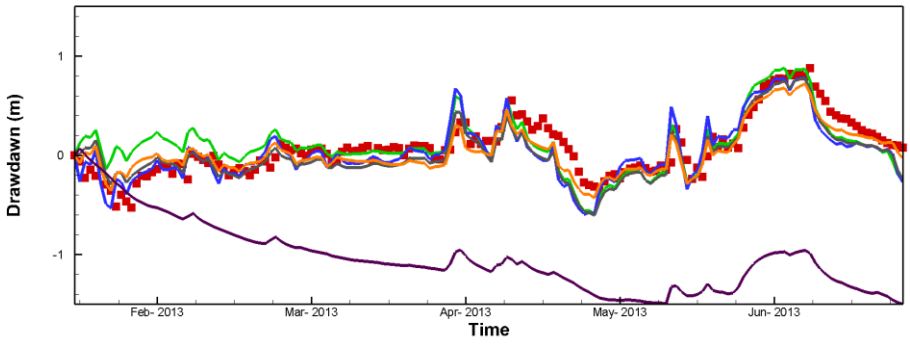

ow8a-89

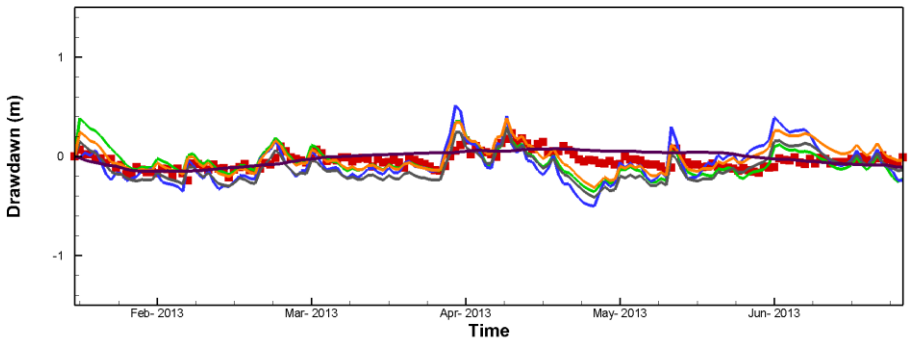

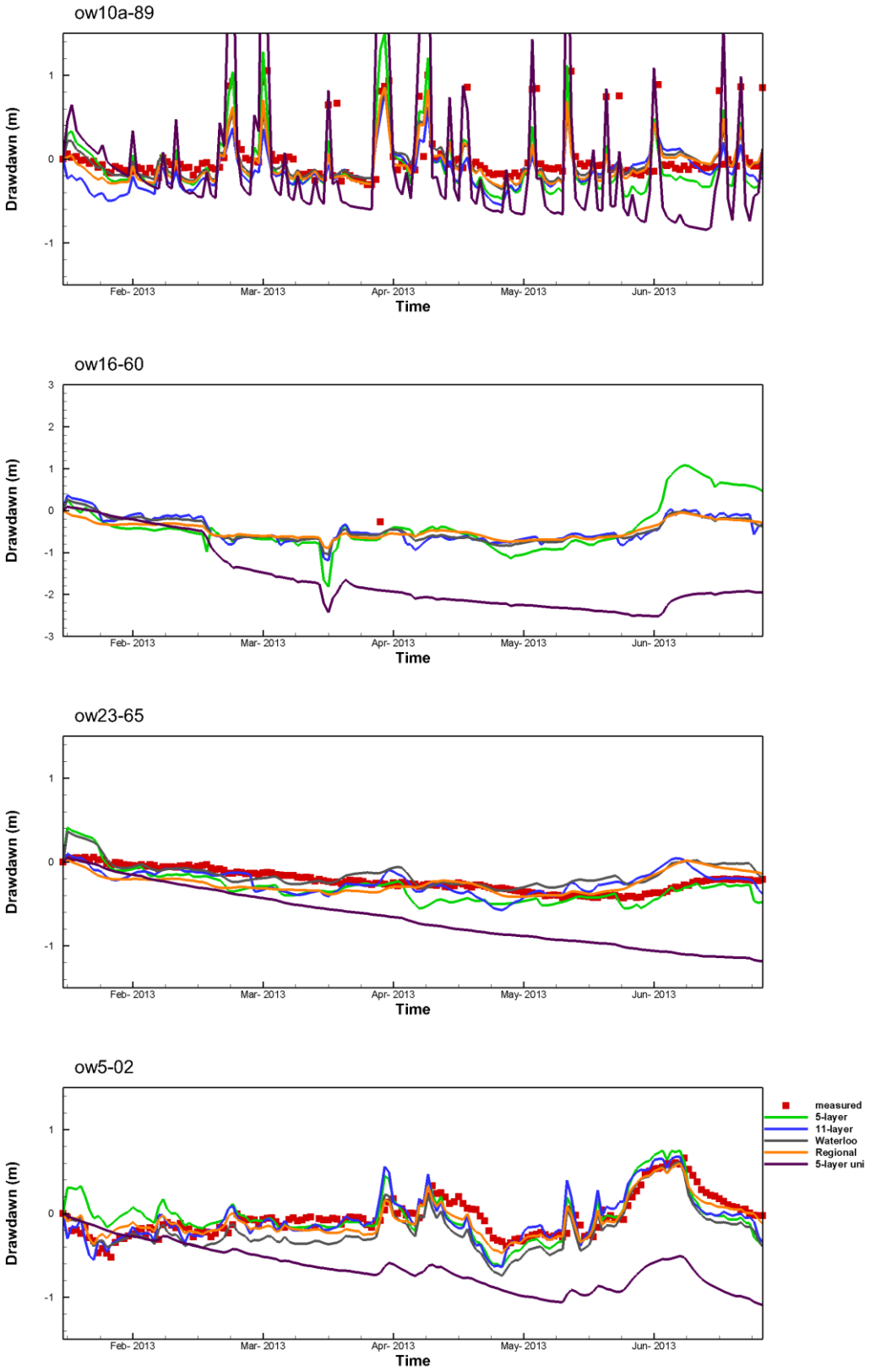
ow10a-89
Drawdawn (m)
1
0
-1
Feb- 2013
Mar- 2013
Apr- 2013
May- 2013
Jun- 2013
Time
ow16-60
Drawdawn (m)
3
2
1
0
-1
-2
-3
Feb- 2013
Mar- 2013
Apr- 2013
May- 2013
Jun- 2013
Time
ow23-65
Drawdawn (m)
1
0
-1
Feb- 2013
Mar- 2013
Apr- 2013
May- 2013
Jun- 2013
Time
ow5-02
Drawdawn (m)
1
0
-1
Feb- 2013
Mar- 2013
Apr- 2013
May- 2013
Jun- 2013
Time
measured
5-layer
11-layer
Waterloo
Regional
5-layer uni

Appendix D. Drawdown versus time for model validation including measured drawdown, simulated drawdown for five cases.

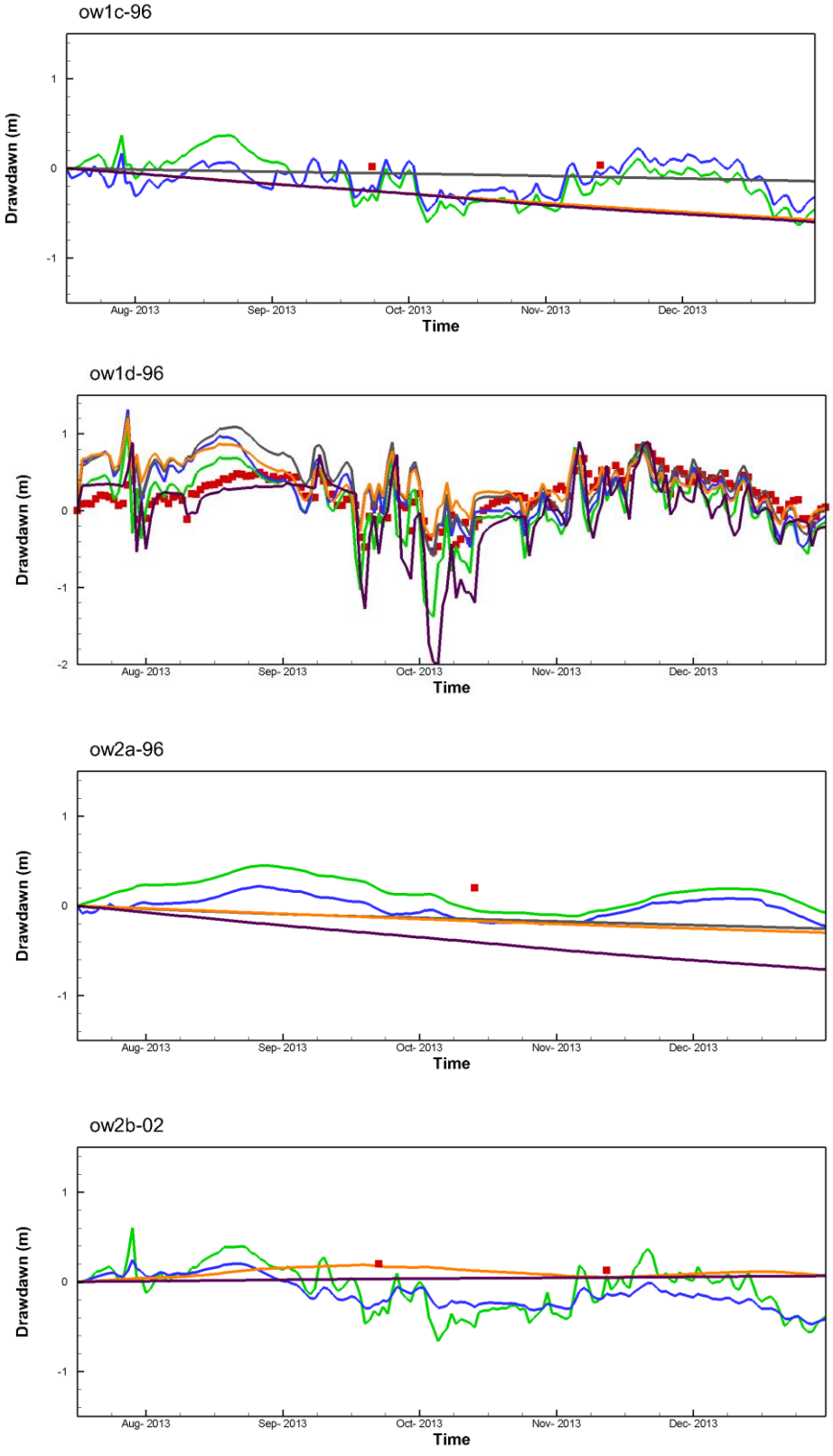

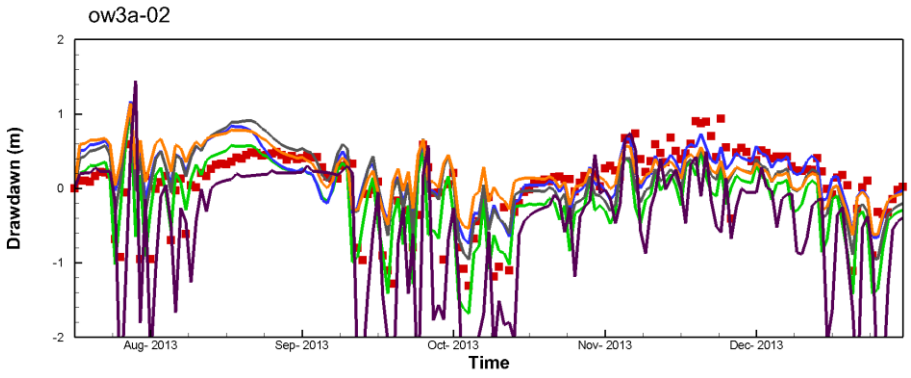
ow3a-02
Drawdawn (m)
2
1
0
-1
-2
Aug- 2013
Sep- 2013
Oct- 2013
Nov- 2013
Dec- 2013
Time

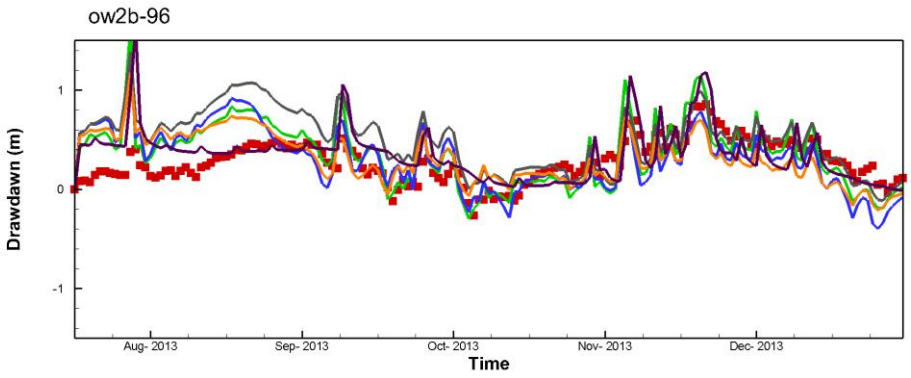
ow2b-96
Drawdawn (m)
1
0
-1
Aug- 2013
Sep- 2013
Oct- 2013
Nov- 2013
Dec- 2013
Time

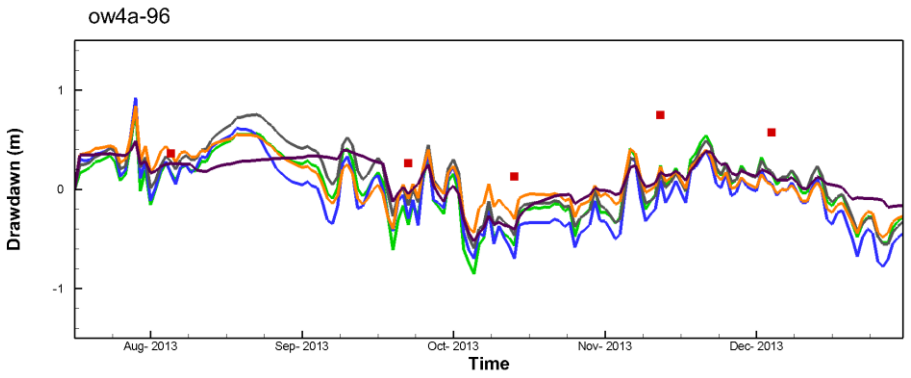
ow4a-96
Drawdawn (m)
1
0
-1
Aug- 2013
Sep- 2013
Oct- 2013
Nov- 2013
Dec- 2013
Time

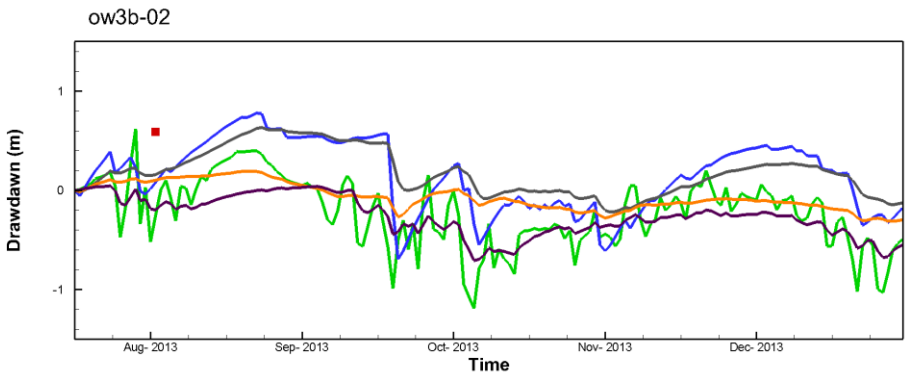
ow3b-02
Drawdawn (m)
1
0
-1
Aug- 2013
Sep- 2013
Oct- 2013
Nov- 2013
Dec- 2013
Time

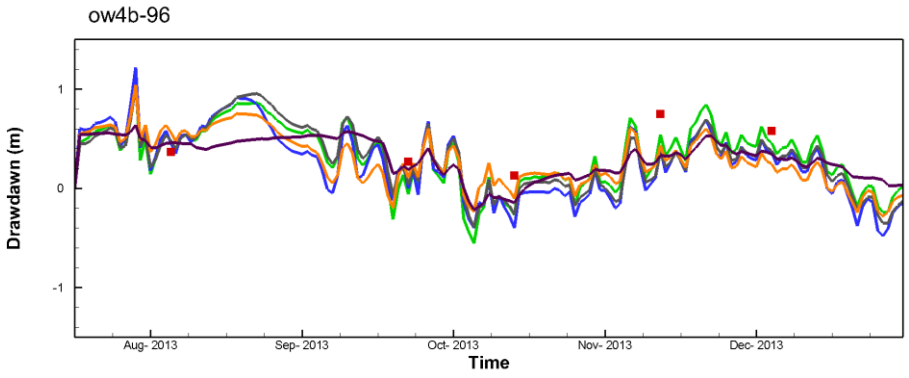
ow4b-96
Drawdawn (m)
1
0
-1
Aug- 2013
Sep- 2013
Oct- 2013
Nov- 2013
Dec- 2013
Time

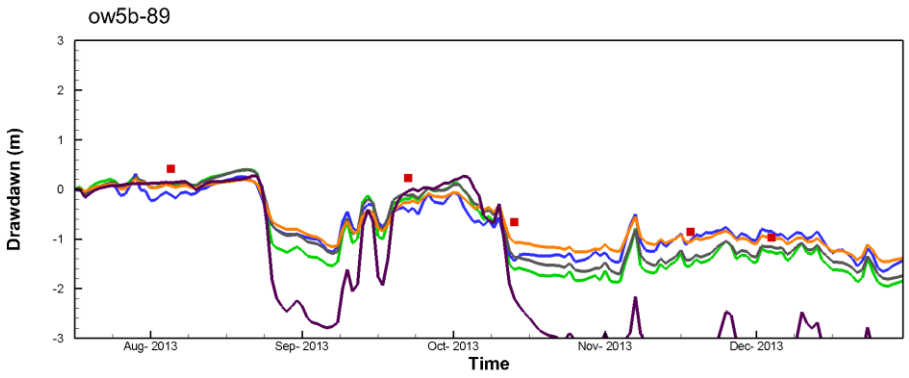
ow5b-89
Drawdawn (m)
3
2
1
0
-1
-2
-3
Aug- 2013
Sep- 2013
Oct- 2013
Nov- 2013
Dec- 2013
Time

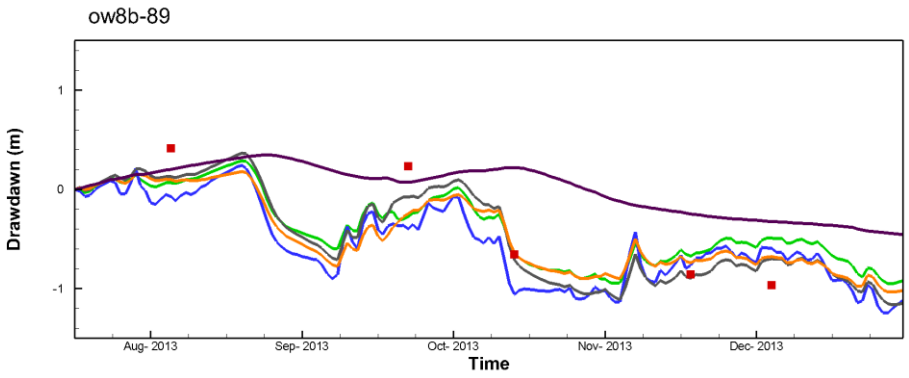
ow8b-89
Drawdawn (m)
1
0
-1
Aug- 2013
Sep- 2013
Oct- 2013
Nov- 2013
Dec- 2013
Time

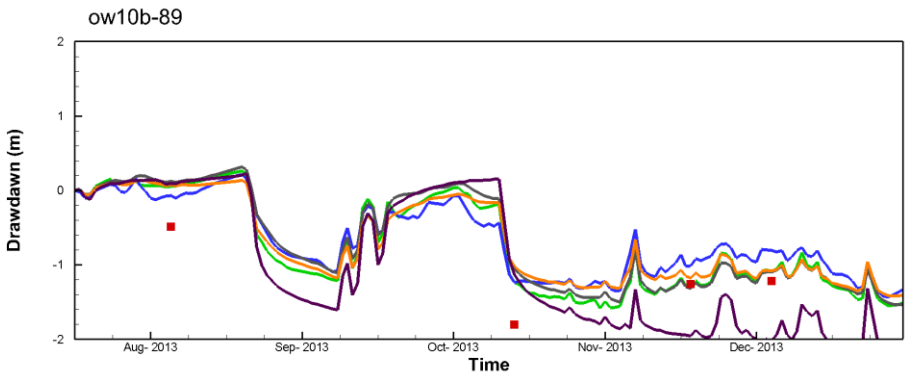
ow10b-89
Drawdawn (m)
2
1
0
-1
-2
Aug- 2013
Sep- 2013
Oct- 2013
Nov- 2013
Dec- 2013
Time

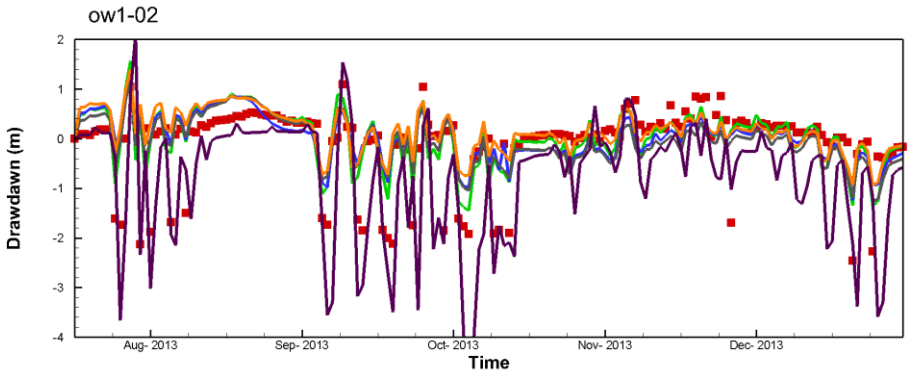
ow1-02
Drawdawn (m)
2
1
0
-1
-2
-3
-4
Aug- 2013
Sep- 2013
Oct- 2013
Nov- 2013
Dec- 2013
Time

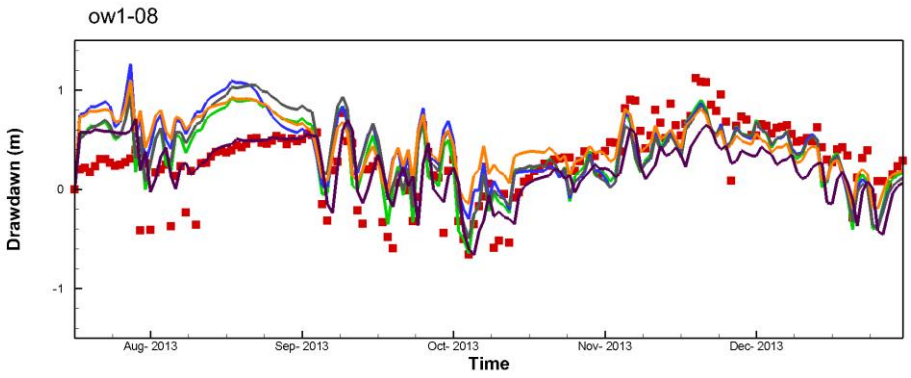
ow1-08
Drawdawn (m)
1
0
-1
Aug- 2013
Sep- 2013
Oct- 2013
Nov- 2013
Dec- 2013
Time

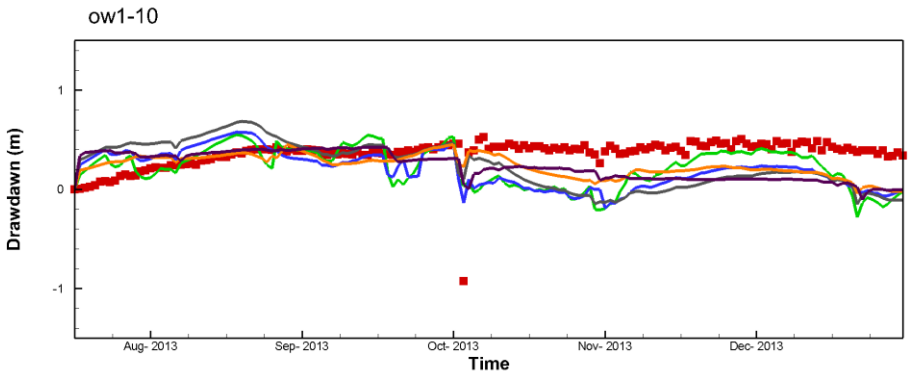
ow1-10
Drawdawn (m)
1
0
-1
Aug- 2013
Sep- 2013
Oct- 2013
Nov- 2013
Dec- 2013
Time

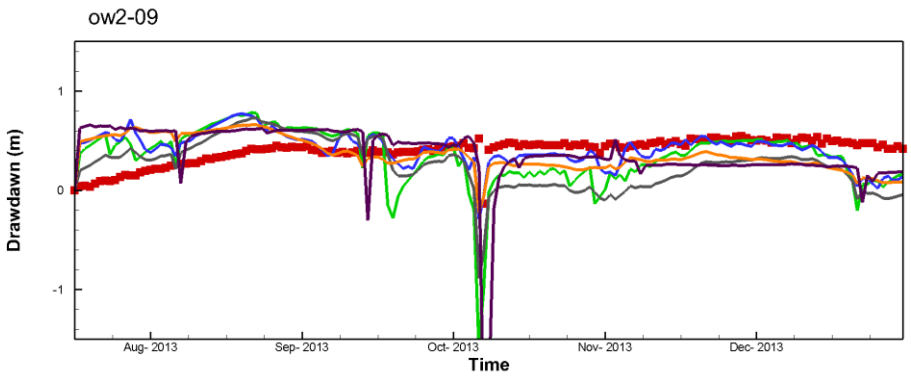
ow2-09
Drawdawn (m)
1
0
-1
Aug- 2013
Sep- 2013
Oct- 2013
Nov- 2013
Dec- 2013
Time

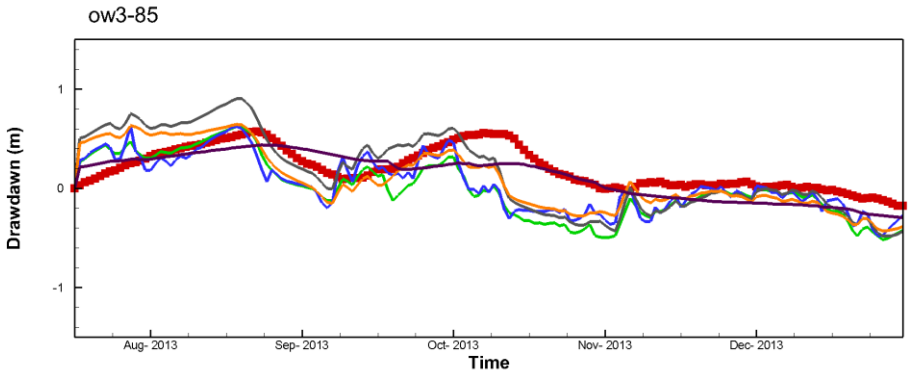
ow3-85
Drawdawn (m)
1
0
-1
Aug- 2013
Sep- 2013
Oct- 2013
Nov- 2013
Dec- 2013
Time

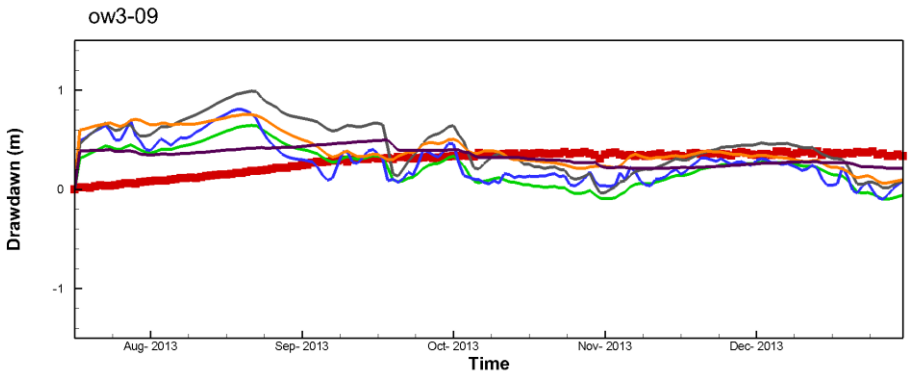
ow3-09
Drawdawn (m)
1
0
-1
Aug- 2013
Sep- 2013
Oct- 2013
Nov- 2013
Dec- 2013
Time

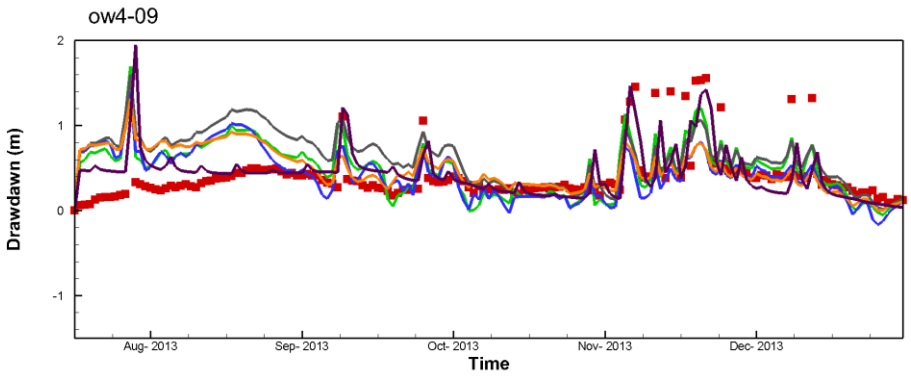
ow4-09
Drawdawn (m)
2
1
0
-1
Aug- 2013
Sep- 2013
Oct- 2013
Nov- 2013
Dec- 2013
Time

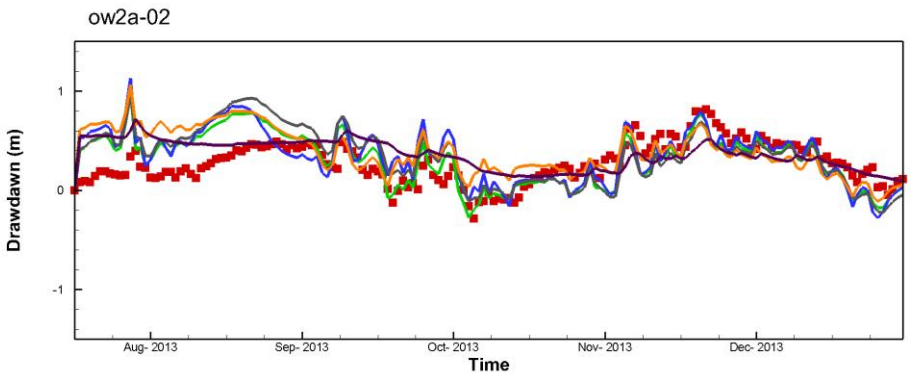
ow2a-02
Drawdawn (m)
1
0
-1
Aug- 2013
Sep- 2013
Oct- 2013
Nov- 2013
Dec- 2013
Time

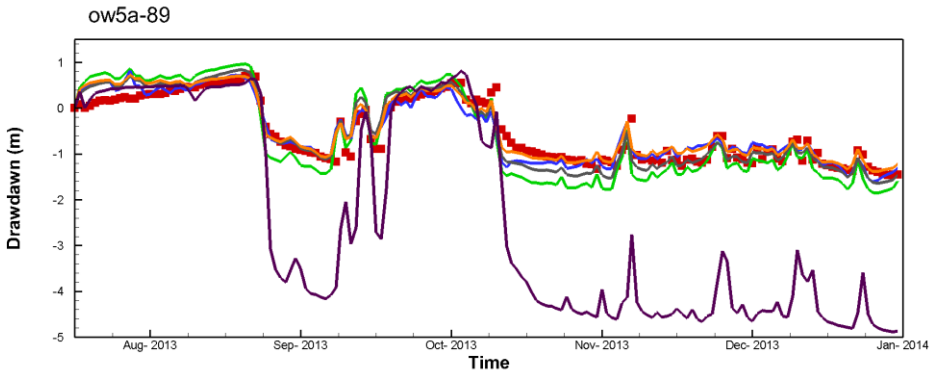
ow5a-89
Drawdawn (m)
1
0
-1
-2
-3
-4
-5
Aug- 2013
Sep- 2013
Oct- 2013
Nov- 2013
Dec- 2013
Jan- 2014
Time

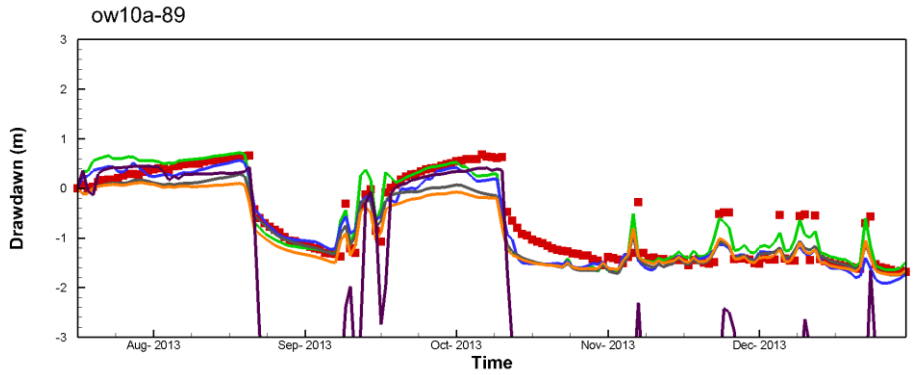
ow10a-89
Drawdawn (m)
3
2
1
0
-1
-2
-3
Aug- 2013
Sep- 2013
Oct- 2013
Nov- 2013
Dec- 2013
Time

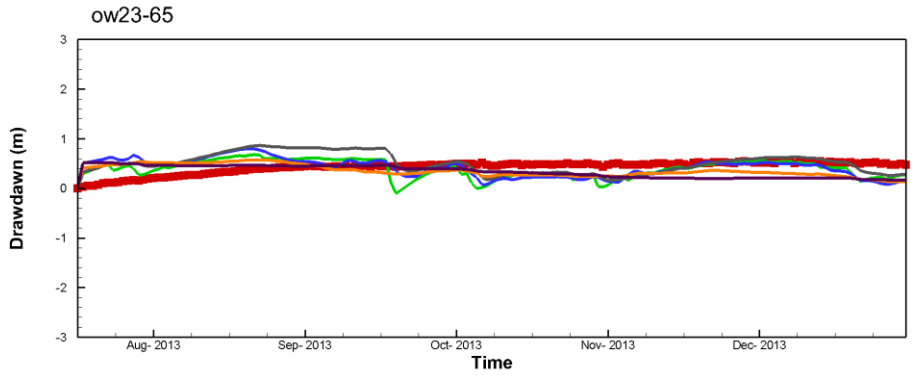
ow23-65
Drawdawn (m)
3
2
1
0
-1
-2
-3
Aug- 2013
Sep- 2013
Oct- 2013
Nov- 2013
Dec- 2013
Time

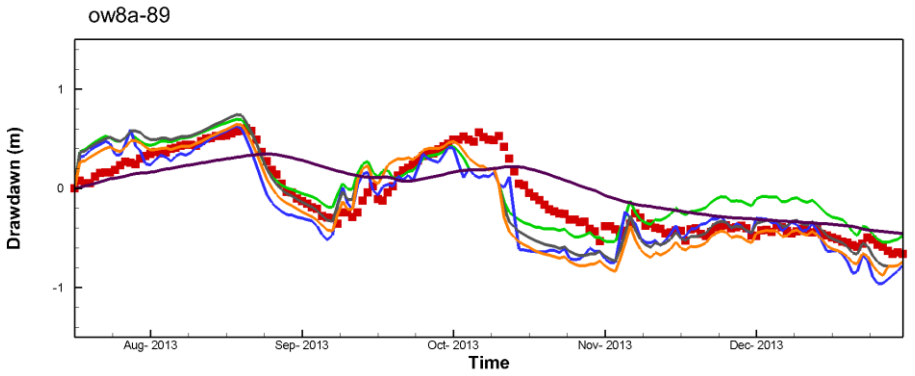
ow8a-89
Drawdawn (m)
1
0
-1
Aug- 2013
Sep- 2013
Oct- 2013
Nov- 2013
Dec- 2013
Time

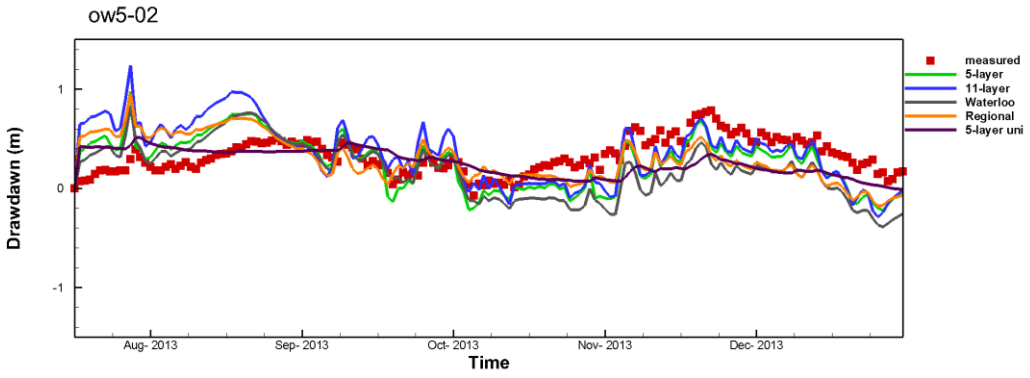
ow5-02
Drawdawn (m)
1
0
-1
Aug- 2013
Sep- 2013
Oct- 2013
Nov- 2013
Dec- 2013
Time
measured
5-layer
11-layer
Waterloo
Regional
5-layer uni